Molecular Biology of the Cell
Vol. 7, 1835–1855, November 1996

Nuclear Transport Defects and Nuclear Envelope Alterations Are Associated with Mutation of the *Saccharomyces cerevisiae NPL4* Gene

Caryn DeHoratius* and Pamela A. Silver†‡

*Department of Molecular Biology, Princeton University, Princeton, New Jersey 08544; and
†Department of Biological Chemistry and Molecular Pharmacology, Harvard Medical School, and the Dana-Farber Cancer Institute, Boston, Massachusetts 02115

Submitted May 24, 1996; Accepted August 28, 1996
Monitoring Editor: Randy W. Schekman

To identify components involved in nuclear protein import, we used a genetic selection to isolate mutants that mislocalized a nuclear-targeted protein. We identified temperature-sensitive mutants that accumulated several different nuclear proteins in the cytoplasm when shifted to the semipermissive temperature of 30°C; these were termed *npl* (nuclear protein localization) mutants. We now present the properties of yeast strains bearing mutations in the *NPL4* gene and report the cloning of the *NPL4* gene and the characterization of the Npl4 protein. The *npl4-1* mutant was isolated by the previously described selection scheme. The second allele, *npl4-2*, was identified from an independently derived collection of temperature-sensitive mutants. The *npl4-1* and *npl4-2* strains accumulate nuclear-targeted proteins in the cytoplasm at the nonpermissive temperature consistent with a defect in nuclear protein import. Using an in vitro nuclear import assay, we show that nuclei prepared from temperature-shifted *npl4* mutant cells are unable to import nuclear-targeted proteins, even in the presence of cytosol prepared from wild-type cells. In addition, *npl4-2* cells accumulate poly(A)$^+$ RNA in the nucleus at the nonpermissive temperature, consistent with a failure to export mRNA from the nucleus. The *npl4-1* and *npl4-2* cells also exhibit distinct, temperature-sensitive structural defects: *npl4-1* cells project extra nuclear envelope into the cytoplasm, whereas *npl4-2* cells form nuclear envelope herniations that appear to be filled with poly(A)$^+$ RNA. The *NPL4* gene encodes an essential M_r 64,000 protein that is located at the nuclear periphery and localizes in a pattern similar to nuclear pore complex proteins. Taken together, these results indicate that this gene encodes a novel nuclear pore complex or nuclear pore complex-associated component required for nuclear membrane integrity and nuclear transport.

INTRODUCTION

Macromolecules enter and exit the nucleus via the nuclear pore complex (NPC), a large structure embedded in the double membrane bilayers of the nuclear envelope (reviewed in Goldberg and Allen, 1995). In recent years, a general picture of how proteins enter the nucleus, how RNAs leave the nucleus, and the composition of the NPC has emerged. Many proteins involved in these processes have been identified, including proteins of the cytoplasm (reviewed in Powers and Forbes, 1994; Sweet and Gerace, 1995), nucleoplasm, and NPC (reviewed in Rout and Wente, 1994; Davis, 1995). Both biochemical and genetic approaches have been invaluable in these searches, and the yeast *Saccharomyces cerevisiae* has proven particularly useful, given the high degree of conservation in NPC proteins (Rout and Blobel, 1993) and soluble transport factors (Sweet and Gerace, 1995).

‡ Corresponding author: Dana-Farber Cancer Institute, 44 Binney Street, Boston, MA 02115.

Studies of mammalian and yeast mutant cells and reconstituted in vitro import reactions have outlined the nuclear protein import pathway (reviewed in Melchior and Gerace, 1995b; Görlich and Mattaj, 1996). In the initial steps of nuclear import, a nuclear localization signal (NLS)-containing substrate binds to an α NLS receptor subunit (karyopherin α/Kap60p) (Görlich *et al.*, 1995; Moroianu *et al.*, 1995a; Rexach and Blobel, 1995), which binds to a β NLS receptor subunit (karyopherin β/Kap95p) (Rexach and Blobel, 1995; Görlich and Mattaj, 1996). The α/β subunits and substrate dock at GLFG or XFXFG repeat-containing NPC proteins (Iovine *et al.*, 1995; Moroianu *et al.*, 1995b; Radu *et al.*, 1995a; Rexach and Blobel, 1995) via the β subunit (Görlich *et al.*, 1995; Moroianu *et al.*, 1995b; Rexach and Blobel, 1995). In subsequent steps, a GTPase (Ran/Gsp1p) (Melchior *et al.*, 1993; Moore and Blobel, 1993; Schlenstedt *et al.*, 1995a) docks at the NPC (Yokoyama *et al.*, 1995), where rounds of GTP hydrolysis (Melchior *et al.*, 1993, 1995) and GDP/GTP exchange (Nehrbass and Blobel, 1996) are mediated by GTPase-activating proteins (RanGAP1/Rna1p and RanBP1/Yrb1p) (Coutavas *et al.*, 1993; Butler and Wolfe, 1994; Bischoff *et al.*, 1995a,b; Corbett *et al.*, 1995; Schlenstedt *et al.*, 1995b) and an accessory protein (p10/NTF2p) (Moore and Blobel, 1994; Paschal and Gerace, 1995). These cycles of hydrolysis and exchange result in the association and dissociation of a Ran/Gsp1–p10/NTF2p–α/β subunits–substrate complex (Nehrbass and Blobel, 1996) that is thought in one hypothesis to travel along an array of docking sites (Radu *et al.*, 1995b; Nehrbass and Blobel, 1996) through the NPC channel. The α subunit, substrate, and Ran/Gsp1p enter the nucleus, while the β subunit and p10/NTF2p remain at the NPC (Görlich *et al.*, 1995; Moroianu *et al.*, 1995b; Corbett and Silver, 1996). The substrate is released inside the nucleus, and the GDP/GTP exchange factor (RCC1/Prp20p) (Aebi *et al.*, 1990; Bischoff and Ponstingl, 1991; Fleischmann *et al.*, 1991) facilitates the GDP/GTP exchange of Ran/Gsp1p; then the α subunit recycles back to the cytoplasm (Koepp *et al.*, 1996).

RNA export also occurs at the NPC and appears to use Ran/Gsp1p and its cofactors (reviewed in Izzurralde and Mattaj, 1995; Görlich and Mattaj, 1996). Mutations in the yeast genes *NUP1*, *GSP1*, *YRB1*, *RNA1*, and *PRP20* and the mammalian gene *RCC1* cause defects in protein import and RNA export (Hopper *et al.*, 1990; Amberg *et al.*, 1992, 1993; Kadowaki *et al.*, 1993; Bogerd *et al.*, 1994; Tachibana *et al.*, 1994; Corbett *et al.*, 1995; Schlenstedt *et al.*, 1995a,b; Koepp *et al.*, 1996). Yet, the mechanisms of protein import and RNA export appear to be distinct. Mutations in the yeast genes *SRP1/KAP60*, *RSL1/KAP95*, and *NTF2* cause protein import defects (Loeb *et al.*, 1995; Corbett and Silver, 1996; Koepp *et al.*, 1996), whereas mutation or deletion of *NUP133/RAT3*, *NUP159/RAT7*, *NUP82*, *NUP120/RAT2*, and *NUP85/RAT9* cause only RNA export defects (Doye *et al.*, 1994; Aitchison *et al.*, 1995a; Gorsch *et al.*, 1995; Grandi *et al.*, 1995; Heath *et al.*, 1995; Hurwitz and Blobel, 1995; Li *et al.*, 1995; Goldstein *et al.*, 1996), and certain mutations in *NUP49* cause either import or export defects (Doye *et al.*, 1994). Nup100p, Nup116p, and Nup145p contain overlapping and essential nucleoporin RNA-binding motifs (NRM) which bind RNA in vitro and may be directly involved in export (Fabre *et al.*, 1994). In addition, human and yeast NPC-associated proteins interact with human immunodeficiency virus type 1 (HIV-1) Rev protein and may be involved in Rev-mediated RNA export (Bogerd *et al.*, 1994; Fritz *et al.*, 1995; Stutz *et al.*, 1995).

Several yeast NPC proteins have also been implicated in maintaining nuclear structure. Partial deletion of *NUP1* induces nuclear envelope projections (Bogerd *et al.*, 1994), and partial deletion of *NUP145* induces NPC clusters (Wente and Blobel, 1994). Deletion or mutation of *NUP133/RAT3*, *NUP120/RAT2*, or *NUP84* results in NPC clustering, whereas deletion or mutation of *NUP85/RAT9* results in NPC clustering and nuclear envelope projections (Doye *et al.*, 1994; Aitchison *et al.*, 1995a; Heath *et al.*, 1995; Li *et al.*, 1995; Goldstein *et al.*, 1996; Siniossogiou *et al.*, 1996), and mutation of *RAT7/NUP159* results in NPC clustering (Gorsch *et al.*, 1995). Deletion of *NUP116* causes formation of intranuclear annulate lamellae and formation of nuclear envelope herniations (Wente and Blobel, 1993). Partial deletion or mutation of *NUP188* causes formation of nuclear envelope blisters (Nehrbass *et al.*, 1996; Zabel *et al.*, 1996), and deletion of *NUP188* in combination with depletion of *POM152* causes prominent projections and invaginations of the nuclear envelope (Nehrbass *et al.*, 1996). Depletion of Nup170p results in enlargement and distortion of the nuclear envelope, whereas overexpression of Nup170p results in formation of intranuclear annulate lamellae (Aitchison *et al.*, 1995b). Thus, NPC proteins are intimately involved in both nuclear transport and structure.

The completed picture of the NPC composition is rapidly emerging. Yeast NPCs have an estimated mass of 66 MDa and contain about 80 proteins (Rout and Blobel, 1993). More than 18 of these proteins have been identified, and more are poised for discovery in isolated yeast NPCs, synthetic lethal screens, and the genome sequencing project. Several years ago, this laboratory initiated several "forward" genetic screens to identify NPC or cytoplasmic proteins involved in nuclear transport (Sadler *et al.*, 1989; Bossie *et al.*, 1992). The screen for nuclear protein localization (*npl*) mutants made use of the missorting of a normally nuclear-targeted protein to the mitochondria. Mutants were selected on the basis of uptake of SV40 NLS-$F_1\beta$-ATPase into the mitochondria at a semipermissive temperature (30°C) and subsequently screened for

failure to grow at the nonpermissive temperature (36°C). Several *NPL* genes have been further characterized. *NPL1* encodes the membrane protein Sec63p, which is involved in endoplasmic reticulum (ER) protein translocation (Rothblatt *et al.*, 1989; Sadler *et al.*, 1989) and nuclear fusion (Ng and Walter, 1996). The role of Npl1p/Sec63p in nuclear transport is not understood, but recent evidence indicates that the secretory protein Sec13p is involved in nuclear pore biogenesis (Siniossogiou *et al.*, 1996), suggesting that specific components may play roles in both ER and NPC structure and/or function. *NPL3* encodes an RNA binding protein (Anderson *et al.*, 1993) that shuttles in and out of the nucleus (Flach *et al.*, 1994). *Npl3* mutants are defective for protein import and mRNA export (Bossie *et al.*, 1992; Kadowaki *et al.*, 1992; Schlenstedt *et al.*, 1993; Wilson *et al.*, 1994; Henry *et al.*, 1996; Lee *et al.*, 1996), indicating that Npl3p may be involved in both processes.

We now report the further characterization of *NPL4*. The *npl4-1* allele was originally isolated in the screen for *npl* mutants described above (Bossie *et al.*, 1992). We later identified *npl4-2*, an additional temperature-sensitive allele. *Npl4* cells show defects in nuclear protein import and poly(A)$^+$ RNA export at the nonpermissive temperature. In addition, *npl4* mutants show defects in nuclear envelope structure, *npl4-1* cells display nuclear envelope projections, and *npl4-2* cells exhibit multiple nuclear herniations containing poly(A)$^+$ RNA. *NPL4* encodes a M_r 64,000 protein that localizes at the nuclear rim in a pattern similar to NPC proteins, consistent with its roles in nuclear transport and structure.

MATERIALS AND METHODS

Genetic Analysis of npl4-1 and npl4-2

The yeast strains used in this study are described in Table 1. Media were prepared as described (Rose *et al.*, 1990; Kassir and Simchen, 1991). Yeast strains were transformed using the Li-acetate method (Ito *et al.*, 1983; Gietz *et al.*, 1992). The *npl4-1* Ts$^-$ strain (PSY108) was isolated as described previously (Bossie *et al.*, 1992). To demonstrate that the *npl4-1* Ts$^-$, Gly$^+$, and nucleolar antigen and histone protein mislocalization phenotypes are due to a single, recessive mutation, *npl4-1* was backcrossed to its wild-type parent strain (PSY78). The diploid was tested for Ts$^+$, sporulated, and used to dissect tetrads. Eight tetrads were tested for Ts$^-$; four of these tetrads were tested for Gly$^+$ and nucleolar antigen and histone protein mislocalization. To determine whether *npl4-1* defines a new complementation group, the *npl4-1* Ts$^-$ strain (PSY108) was crossed to several well-characterized Ts$^-$ strains, including *sec61-2*, *sec62-1*, *sec63-101*/*npl1-1*, *npl3-1*, and *npl6-1* (Deshaies and Schekman, 1987, 1989; Rothblatt *et al.*, 1989; Sadler *et al.*, 1989; Bossie *et al.*, 1992; Chiang, 1993). In each case, the resulting diploid was tested for Ts$^+$. To establish that *npl4-1* (PSY109) is allelic to the Ts$^-$ strain (PSY824) (Klyce and McLaughlin, 1973), both Ts$^-$ strains were outcrossed with the same wild-type strain (FY86), and the outcrossed strains were mated. The resulting diploid was tested for Ts$^-$, sporulated, and used to dissect tetrads. Twenty-four tetrads were tested for Ts$^-$. To investigate genetic interactions between *NPL4* and other yeast NPC component-encoding genes, *npl4-1* (PSY825) and *npl4-2* (PSY826) strains were crossed to Δ*nup100-3*, Δ*nup145-7*, Δ*nup116-5*, *rat3-1*, *rat7-1*, *rat8-1*, *rat9-1*, and Δ*pom152* strains (Wente and Blobel, 1994; Aitchison *et al.*, 1995a,b; Gorsch *et al.*, 1995; Li *et al.*, 1995; Goldstein *et al.*, 1996; Cole, unpublished data). In each case, the resulting diploid was tested for Ts$^+$, sporulated, and used to dissect tetrads.

Molecular Analysis of NPL4

The plasmids used in this study are described in Table 2. To clone *NPL4*, the *npl4-1* Ts$^-$ strain was transformed with a single-copy *URA3*-based yeast genomic library (Rose *et al.*, 1987), plated onto uracil drop-out plates, and incubated at 36°C. The resulting Ts$^+$, Ura$^+$ colonies were checked for reversion to Ts$^-$, Ura$^-$ after plasmid loss. The Ts$^+$, Ura$^+$ strains were then used to isolate plasmid DNA (pPS404). The DNA was used to transform the original *npl4-1* strain, and the tranformants were tested for Ts$^+$ and Ura$^+$. To demonstrate that the *npl4-1* Ts$^-$ phenotype is linked to the *NPL4* gene, a *URA3*-based plasmid carrying a *Bam*HI-*Eco*RI ~1-kb fragment of the cloned genomic DNA insert (pPS805) was integrated into a wild-type strain (W303). Integration was confirmed by Southern blot analysis, and the *NPL4::URA3* strain (PSY826) was crossed to *npl4-1* (PSY894). The diploid was sporulated and used to dissect tetrads. Twenty-two tetrads were tested for Ts$^-$ and Ura$^+$.

To determine the minimal complementing region of the cloned genomic DNA insert, the cloned DNA (pPS404) was used to make *Dra*I, *Nru*I, and *Xba*I deletion constructs, and the *Dra*I ~2-kb fragment was subcloned into YCp50 (pPS402). The deletion constructs and the *Dra*I construct were transformed into *npl4-1*, and the transformants were tested for Ts$^+$. The *Dra*I fragment was sequenced (Sanger *et al.*, 1977) and used to determine the *NPL4* coding region. To disrupt *NPL4*, a *Bam*HI-*Pst*I fragment of *LEU2* (pJJ252) (Jones and Prakash, 1990) was inserted into the *Bam*HI-*Pst*I deletion of *NPL4* (pPS798); the construct deleted Npl4p amino acids 94–539. The *npl4::LEU2* fragment was isolated and integrated into a wild-type diploid strain (RKY1154). Integration was confirmed by Southern blot analysis, and the Δ*npl4* diploid was sporulated; 19 tetrads were dissected and tested for Leu$^-$. The Δ*npl4* diploid was transformed with a plasmid carrying *NPL4* and *URA3* (pP800), and the transformants were sporulated. Four tetrads were tested for Leu$^+$ and Ura$^+$ and the ability to grow on 5-flouroorotic acid (5-FOA).

The *npl4* Ts$^-$ mutations were cloned as described (Orr-Weaver and Szostak, 1983). The original *NPL4* plasmid (pPS404) was digested with *Dra*I, and the gapped plasmid DNA was used to transform the *npl4-1* (PSY825) and *npl4-2* (PSY826) strains. The resulting Ura$^+$ colonies were tested for Ts$^-$ and used to isolate plasmid DNA. The *npl4-1* (pPS801) and *npl4-2* (pPS802) plasmid DNAs were used to transform the Δ*npl4* diploid (PSY828) strain. The diploid transformants were used to sporulate and dissect tetrads and tested for Ura$^+$ and Ts$^-$. To test for rescue of the *npl4* Ts$^-$ defect, the *npl4-1* (PSY825) and *npl4-2* (PSY826) strains were transformed with plasmids containing high-copy *NUP116* (pCP29), and transformants were plated on uracil drop-out plates at room temperature (RT) and 36°C. To test for rescue of the Δ*nup116* Ts$^-$ defect, the Δ*nup116* (SWY27) strain was transformed with plasmids containing single-copy *URA3* and *NPL4* (pPS402), high-copy *URA3* and *NPL4* (pPS806), *URA3* and *GAL1* promoter *NPL4* (pPS807), single-copy *URA3* and *NUP116* (SWY127), and vector (YEp24). The Δ*nup116* transformants and a Ura$^-$ wild-type strain (FY86) were plated on 5-FOA plates and uracil drop-out plates containing 2% glucose, 1.5% glucose, 0.5% galactose, and 2% galactose and incubated at RT and at 36°C.

Preparation of Antibodies to Npl4p

The *NPL4 Sal*I-*Pst*I fragment encoding amino acids 39–407 was inserted into pMal-c2 (New England Biolabs, Beverly, MA) to make a maltose binding protein fusion construct (pPS803). The *MBP-NPL4* construct was transformed into HB101, the protein was induced in 0.3 mM isopropyl thiogalactoside for 1 h at RT, soluble

Table 1. Yeast strains used in this study

Strain	Genotype	Source
Dat3-2	*Mat a leu2Δ1 trp1 Δ63 ura3-52 rat3-1*	Li *et al.*, 1995
FY86	*Mat α leu2-Δ1 his3-Δ200 ura3-52*	Winston, unpublished data
PSY78	*Mat α gal2 his4-519 leu2-3,112 suc2-Δ9 ura3-52 Δatp2::LEU2*	Emr *et al.*, 1986
PSY108	*Mat a leu2-3,112 lys2-801 suc2-Δ9 trp1-Δ901 ura3-52 Δatp2::LEU2* carrying pPS345	this lab
PSY824	*Mat a ade1 ade2 his4 lys2 trp1 ura1 npl4-2*	Klyce and McLaughlin, 1973
PSY825	*Mat a leu2 ura3-52 npl4-1*	this study
PSY826	*Mat a his3-Δ200 ura3-52 npl4-2*	this study
PSY827	*Mat a ade2-1 can1-100 his3-1,115 leu2-3 trp1-1 ura3-1 NPL4::URA3*	this study
PSY828	*Mat a/α Δho::hisG/Δho::hisG Δleu2::hisG/Δleu2::hisG lys2/lys2 ura3/ura3 Δnpl4::LEU2/NPL4*	this study
PSY894	*Mat α leu2 ura3 npl4-1*	this study
RKY1154	*Mat a/α Δho::hisG/Δho::hisG Δleu2::hisG/Δleu2::hisG lys2/lys2 ura3/ura3*	Kolodner, unpublished data
SWY27	*Mat α ade2-1 can1-100 his3-1 leu2-3 trp1-1 Δnup116::HIS3*	Wente and Blobel, 1993
SWY127	*Mat α ade2-1 can1-100 his3-1 leu2-3 trp1-1 Δnup116::HIS3* carrying pSW131 *(CEN/NUP116/URA3)*	Wente and Blobel, 1994
W303	*Mat a ade2-1 can1-100 his3-11,15 leu2-3 trp1-1 ura3-1*	Thomas and Rothstein, 1989

protein was extracted and purified on an amylose resin column (New England Biolabs), the purified fraction was resolved by SDS-PAGE (Laemmli, 1970), and the band specific for isopropyl thiogalactoside induction was excised, homogenized, and injected with Freund's adjuvant into a New Zealand White rabbit (HRP, Denver, PA). The resulting polyclonal antibodies were affinity purified as follows. The *NPL4 Bam*HI fragment encoding amino acids 94–580 was inserted into pGEX-2T (Pharmacia Biotech, Picscataway, NJ) to make a glutathione *S*-transferase fusion construct (pPS805). The glutathione *S*-transferase-*NPL4* construct was transformed into HB101; the protein was induced and extracted as described above and purified on a glutathione-Sepharose 4B column (Pharmacia Biotech). The purified fusion protein was coupled to CNBr-activated Sepharose 4B (Sigma Chemical, St. Louis, MO) and used to purify the isolated IgG fraction (Immunopure (G) IgG purification kit; Pierce, Rockford, IL) of the anti-Npl4p serum.

For Western blot analysis of wild-type Npl4p, total cell extracts were prepared from wild-type cells (W303) or wild-type cells transformed with single-copy *NPL4* (pPS402), high-copy *NPL4* (pPS806), or *GAL1* promoter-*NPL4* (pPS807) plasmids. For analysis of wild-type and mutant Npl4p, total cell extracts were prepared from wild-type (FY86), *npl4-1* (PSY825), and *npl4-2* (PSY826) cells grown at RT or shifted to 37°C for 5 h. Immunoblotting was performed as described previously (Bossie *et al.*, 1992), except that blots were incubated with affinity-purified rabbit anti-Npl4p antibodies (1:500) at 4°C for 12 to 18 h, followed by incubation with horseradish perxoidase-labeled anti-rabbit IgG secondary antibodies (1:5000; Promega) at RT for 1 h, and visualized by enhanced chemiluminescence (Amersham, Arlington Heights, IL). Npl4p bands were quantitated using the National Institutes of Health Image program.

For indirect immunofluorescence, wild-type diploid cells (RKY1154) were grown at 30°C in YEPD to A_{600} ~1. Cells were treated as described previously (Sadler *et al.*, 1989) with a number of modifications. Formaldehyde fixation was omitted, and unfixed cells were spheroplasted with 0.02 mg/ml zymolyase at RT for 10 min, incubated in methanol at RT for 6 min, and incubated in acetone at RT for 30 s. Spheroplasts were incubated with affinity-purified rabbit anti-Npl4p antibodies (1:20) at RT for 12 to 18 h, followed by incubation with fluorescein isothiocyanate (FITC)-labeled anti-rabbit IgG secondary antibodies (1:1000; Jackson ImmunoResearch Laboratories, West Grove, PA) at RT for 2 h, and 4′,6-diamidino-2-phenylindole (DAPI). For double labeling, wild-type

Table 2. Plasmids used in this study

Plasmid	Markers	Construction	Source
pCP29	2μ *URA3*	*NUP116* in YEp13	Wente, unpublished data
pJJ252	*LEU2*	*LEU2* in pUC18	Jones and Prakash, 1990
pPS345	2μ *URA3*	*GAL1* promoter, SV40 NLS, *SUC2* in YEp24	this laboratory
pPS402	*CEN4 URA3*	*NPL4 Dra*I fragment in YCp50	this study
pPS404	*CEN4 URA3*	*NPL4* clone in YCp50	this study
pPS798		*NPL4 Sal*I-*XBa*I fragment in Bluescript KS(−)	this study
pPS799		*LEU2 Bam*HI-*Pst*I fragment in pPS798	this study
pPS800	*CEN4 URA3*	*NPL4 Sal*I site inserted with myc in YCp50	this study
pPS801	*CEN4 URA3*	*npl4-1 Xba*I fragment in pPS404	this study
pPS802	*CEN4 URA3*	*npl4-2 Xba*I fragment in pPS404	this study
pPS803		*NPL4 Sal*I-*Pst*I fragment in pMAL-c2	this study
pPS804		*NPL4 Bam*HI fragment in pGEX-2T	this study
pPS805	*URA3*	*NPL4* clone *Bam*HI-*Eco*RI fragment in Ylp5	this study
pPS806	2μ *URA3*	*NPL4 Dra*I fragment in YEp24	this study
pPS807	2μ *URA3*	NPL4 *Cla*I fragment in YEp352	this study

diploid (RKY1154) cells were grown at 30°C in YEPD to A_{600} ~1, or *rat3-1* (Dat3-2) cells were grown at RT in YEPD to A_{600} ~1. Cells were fixed in 4% 1-ethyl-3-(3-dimethyl-aminopropyl) carbodiimide (Pierce Chemical) and treated as described above. Spheroplasts were incubated with affinity-purified rabbit anti-Npl4p antibodies (1:20) and guinea pig anti-Rat7/Nup159p antibodies (1:2000; Gorsch *et al.*, 1995) at RT for 12 to 18 h, followed by incubation with Texas Red-anti-rabbit IgG and FITC-anti-guinea pig IgG secondary antibodies (Jackson ImmunoResearch Laboratories) at RT for 2 h and DAPI.

Protein Import and Retention Assays

To examine the nuclear import of NLS-invertase, wild-type (FY86), *npl4-1* (PSY825), and *npl4-2* (PSY826) cells were transformed with the *GAL1* promoter-SV40 NLS-*SUC2* construct pPS345 (Chiang, 1993). Cells were grown at RT in uracil drop-out media with 2% raffinose to A_{600} ~0.5, shifted to 2% galactose at RT for 3 h, and grown at RT or 37°C for 30 min or 3 h. To examine the nuclear retention of NLS-invertase, cells were transformed and grown as described above, shifted to 2% galactose at RT for 3 h, washed, shifted to 2% glucose at RT for 1 h, and grown at RT or 37°C for 3 h. Following temperature shifts, cells were prepared for immunofluorescence microscopy (Sadler *et al.*, 1989) and incubated with rabbit anti-invertase antibodies (1:20,000; Nelson and Silver, 1989) at RT for 12–18 h, followed by incubation with FITC-labeled anti-rabbit IgG secondary antibodies (1:1000; Jackson ImmunoResearch Laboratories) at RT for 2 h and DAPI.

In Vitro Import Assay

The in vitro nuclear import assay was performed as described elsewhere (Schlenstedt *et al.*, 1993). Wild-type (FY86), *npl4-1* (PSY825), and *npl4-2* (PSY826) cells were grown at RT to A_{600} ~0.4, maintained at RT or shifted to 37°C for 3 h, and used to prepare semi-intact cells and cytosol. Cells were collected by centrifugation, resuspended in 100 mM piperazine-*N*,*N*′-bis(2-ethanesulfonic acid) (PIPES), pH 9.4, 10 mM dithiothreitol, incubated at 30°C for 10 min, and collected by centrifugation. Cells were resuspended in 0.2% glucose, 50 mM KPO_4 (pH 7.5), and 0.6 M sorbitol. Cells were digested with 300 U/ml oxalyticase (40,000 U/ml stock in 50 mM KPO_4, pH 7.5; Enzogenetics, Corvallis, OR) at 30°C for 15 min. Spheroplasts were collected by centrifugation, resuspended in 1% glucose, 0.7 M sorbitol, and incubated at 30°C for 20 min. Spheroplasts were collected by centrifugation, washed twice with 20 mM PIPES-KOH (pH 6.8), 150 mM potassium acetate, 2 mM magnesium acetate, 0.4 M sorbitol, resuspended in this buffer with 0.5 mM EGTA, frozen slowly above liquid N_2, and stored at −80°C.

For the import experiments, spheroplasts were thawed on ice, washed four times with cold buffer A (0.25 M sorbitol, 20 mM PIPES-KOH, pH 6.8, 150 mM potassium acetate, 5 mM magnesium acetate), and resuspended in buffer A. The import reaction mixture contained buffer A (20 mM PIPES/KOH, pH 6.8, 250 mM sorbitol, 150 mM potassium acetate, 5 mM magnesium acetate) with 5×10^7 cells/ml, 5 mg SV40 NLS-HSA-rhodamine conjugate, 1 mM ATP (Sigma Chemical), 10 mM creatine phosphate (Boehringer Mannheim, Indianapolis, IN), 0.1 mg/ml creatine-kinase (Boehringer Mannheim), and 1.5 mg/ml cytosolic proteins. Reactions were incubated in the dark at 30°C for 10 min. Cells were mixed with DAPI (final concentration, 0.25 mg/ml) and analyzed by fluorescence microscopy. For each reaction, ~200-300 cells were assayed for permeability (DAPI staining) and import (nuclear accumulation of substrate).

Poly(A)$^+$ RNA Localization Assay

In situ hybridization of poly(A)$^+$ RNA was performed as described previously (Amberg *et al.*, 1992). Wild-type (FY86), *npl4-1* (PSY825), and *npl4-2* (PSY826) cells were grown at RT in YEPD to A_{600} ~0.5, cells were continued at RT or shifted to 37°C for 30 min, fixed at 37°C for 1.5 h, and washed in solution P (0.1 M KPO_4, pH 6.5, 1.2 M sorbitol). Cells were permeabilized with 0.5% Nonidet P-40 in solution P at RT for 5 min, equilibrated with 0.1 M triethanolamine, pH 8.0, at RT for 2 min, and blocked with 0.25% acetic anhydride in 0.1 M triethanolamine, pH 8.0, at RT for 10 min. Cells were incubated in prehybridization solution (50% deionized formamide, 4× SSC, 1× Denhardt's solution, 10% dextran sulfate, 125 μg/ml tRNA, and 500 μg/ml salmon sperm DNA) at 37°C for 1 h and subsequently incubated in prehybridization solution with oligo(dT)$_{50}$-digoxigenin-labeled probe at 37°C for 12 to 18 h, followed by incubation with FITC-conjugated antidigoxigenin F′ab fragments (1:200; Jackson ImmunoResearch Laboratories) at RT for 2 h and DAPI. Samples were analyzed by fluorescence microscopy.

Electron Microscopy

Cells were prepared for transmission electron microscopy (TEM; McDonald, 1984), with a number of modifications. Wild-type (FY86), *npl4-1* (PSY825), and *npl4-2* (PSY826) cells were grown at RT to A_{600} ~0.04, and cells were maintained at RT or shifted to 37°C for 30 min, 3 h, or 5 h and collected by centrifugation. Cells were washed twice with 40 mM K_2HPO_4-KH_2PO_4, pH 6.5, and 0.5 mM $MgCl_2$, and fixed with 2% glutaraldehyde (70% EM grade stock; Ted Pella, Redding, CA) at RT for 30 min. Cells were washed twice with 0.17 M KH_2PO_4, 30 mM sodium citrate, resuspended in the buffer, and digested with 0.04 mg/ml lyticase (Sigma Chemical) at 30°C for 10 to 15 min. The resulting spheroplasts were washed twice in 0.1 M sodium acetate, pH 6.1, postfixed in 1% osmium tetroxide and 0.5% potassium ferrocyanide at RT for 1 h, rinsed with dH_2O, resuspended in 2% uranyl acetate, and incubated in the dark at 4°C for 12 to 18 h. Samples were washed, dehydrated, embedded in Epon, and sectioned. Sections were stained with lead citrate and uranyl acetate and examined with a JEOL 100CX transmission electron microscope at 60 kV using a 20-μm objective aperture. For each RT, 30-min, 3-h, and 5-h temperature-shift experiment, ~30 micrographs were analyzed for altered morphology. For each RT and 5-h temperature-shift experiment, ~10 micrographs were measured to calculate nuclear and cellular areas. For the isogenic strains, Δ*npl4* cells covered with *NPL4* (pPS404), *npl4-1* (pPS924), and *npl4-2* (pPS925) single-copy plasmids were grown in uracil/leucine drop-out media or YEPD to A_{600} ~0.06 and shifted to 37°C for 5 h. Cells were prepared for TEM as described above. For the plasmid rescue strains, Δ*nup116* cells carrying single-copy *NUP116* (SWY127), high-copy *NPL4* (pPS806) plasmids, and vector (YEp24) were grown in uracil drop-out media to A_{600} ~0.6 and shifted to 34°C for 5 h. Cells were prepared for TEM as described above.

In situ RNA hybridization and electron microscopy were performed as described (Huang *et al.*, 1994). Wild-type (FY86) and *npl4-2* (PSY826) cells were prepared for poly(A)$^+$ RNA in situ hybridization (see above), except that the sample was shifted to 37°C for 3 h and that formamide was omitted from the prehybridization solution. Cells were incubated with or without oligo(dT)$_{50}$-digoxigenin, incubated with antidigoxigenin antibodies conjugated to 0.8 nm gold (Boehringer Mannheim), fixed, and silver enhanced (HQ Silver; Nanoprobes, Stony Brook, NY). Cells were prepared for TEM as described above.

Immunoelectron microscopy was performed by preparing *npl4-2* cells for TEM (see above), except that cells were fixed in 0.1% glutaraldehyde in Zamboni, spheroplasted, embedded into 3% gelatin in phosphate-buffered saline, frozen in liquid N_2, and used to cut thin sections. Thin sections were processed, incubated with MAb414 (1:10; Aris and Blobel, 1989), followed by incubation with anti-mouse IgG conjugated to 10 nm gold (1:20; Jackson ImmunoResearch Laboratories), and examined by TEM as described above. For the frozen sections, ~10 micrographs were used to count gold particles and calculate cytoplasmic, nucleoplasmic, and nuclear envelope herniation base areas.

RESULTS

Genetic Analysis of npl4-1 and npl4-2

We reasoned that *npl* mutants could be identified by screening for Δ*atp2* cells that were transformed with the SV40 NLS-*ATP2* construct but were unable to efficiently translocate the NLS-F1β-ATPase fusion protein into the nucleus. In principle, these cells would redirect the fusion protein to the mitochondria and would thereby be able to respire, i.e., grow on glycerol. We predicted that a partial block in nuclear import would result in the rerouting of the fusion protein and growth on glycerol, whereas a complete block in nuclear import would result in cell death. We, therefore, isolated mutants that were glycerol positive (Gly^+) at 30°C and failed to grow at 36°C (Ts^-). The screen identified one new allele of *NPL1*, six alleles of *NPL3*, one allele of *NPL4*, and a number of single isolates (Bossie *et al.*, 1992). The *npl* mutants were grown continuously at 30°C and tested for the mislocalization of endogenous nucleolar antigens and histone proteins. At the semipermissive temperature, *npl1-6*, *npl3-1*, *npl3-250*, and *npl4-1* cells showed significant cytoplasmic accumulation of these nuclear proteins (Bossie *et al.*, 1992).

More recently, we subjected the *npl4-1* mutant to extensive genetic analysis. To show that the *npl4-1* Ts^-, Gly^+, and the nuclear protein mislocalization phenotypes are due to a single recessive mutation, we backcrossed the original *npl4* isolate (expressing NLS-F_1β-ATPase) to its wild-type parent (see MATERIALS AND METHODS); the resulting diploid was Ts^+, and tetrad analysis showed that the Ts^-, Gly^+, and nuclear protein mislocalization phenotypes were tightly linked. To demonstrate that *npl4-1* does not belong to previously identified complementation groups, we crossed *npl4-1* to *npl1-1/sec63-101*, *npl3-1*, *npl6-1*, *sec61-2*, and *sec62-1* Ts^- strains (see MATERIALS AND METHODS). In all cases, the diploids became Ts^+, indicating that the *npl4-1* strain was able to complement these Ts^- strains. However, the *npl4-1* mutant failed to complement a previously uncharacterized isolate from an independently derived Ts^- collection (Klyce and McLaughlin, 1973). We confirmed that this Ts^- isolate is allelic to *npl4-1* by mating *npl4-1* to this Ts^- isolate (see MATERIALS AND METHODS); the resulting diploid was Ts^-, and tetrad analysis showed that the two Ts^- mutations were tightly linked. The Ts^- isolate was designated *npl4-2*. To investigate whether *npl4-1* and *npl4-2* mutations showed synthetic lethality in combination with previously identified *nup*, *pom*, and *rat* mutations, we crossed the *npl4* strains to several mutant strains and used the resulting diploids to dissect tetrads (see MATERIALS AND METHODS). In all cases, the tetrads showed normal viability, indicating a lack of synthetic lethality.

Cloning the NPL4 Gene

We cloned the *NPL4* gene by transforming the *npl4-1* strain with a single-copy *URA3*-based yeast genomic DNA library (Rose *et al.*, 1987) and selecting for Ts^+, Ura^+ colonies (see MATERIALS AND METHODS). Ten Ura^+, Ts^+ colonies were isolated and used to generate plasmid segregants. Nine of the segregants reverted to Ts^-, and one of these nine transformants was used to isolate plasmid DNA. The DNA was used to retransform the *npl4-1* strain, and this transformant became Ts^+. Deletion constructs localized the *npl4-1* minimal complementing region to a ~2-kb *Dra*I fragment (Figure 1A). This fragment was sequenced to determine the *NPL4* open reading frame (see MATERIALS AND METHODS). The *NPL4* gene corresponds to an open reading frame on chromosome II identified by the yeast genome sequencing project (Schaaff-Gerstenschläger *et al.*, 1993).

To ensure that the *NPL4* cloned fragment is linked to the *npl4-1* Ts^- mutation, we integrated a plasmid carrying a fragment of the *NPL4* cloned insert and *URA3* into a wild-type strain (see MATERIALS AND METHODS). The integration was checked by Southern blot analysis, and the *URA3::NPL4* strain was crossed to *npl4-1* (see MATERIALS AND METHODS). Tetrad analysis showed that the Ts^- and Ura^- phenotypes were tightly linked. This indicated that the cloned fragment contains *NPL4* rather than an unlinked suppressor of *npl4-1*.

To determine whether *NPL4* is an essential gene, we replaced the *NPL4* coding region with *LEU2* in a wild-type diploid strain (Figure 1A; see MATERIALS AND METHODS). The disruption was checked by Southern blot analysis, and the Δ*npl4* diploid was sporulated and used to dissect tetrads. Tetrad analysis showed only two viable spores per tetrad, and all spores were Leu^-. The Δ*npl4* diploid was then transformed with a plasmid carrying *NPL4* and *URA3*, sporulated, and used to analyzed tetrads (see MATERIALS AND METHODS). In this case, tetrad analysis showed four viable spores per tetrad, and the Leu^+ spores were always Ura^+. Furthermore, the Leu^+ spores were unable to grow on 5-FOA, indicating that they were unable to lose the *NPL4*-containing plasmid. These results confirmed that *NPL4* is essential for cell growth. Similar results were obtained by Schaaff-Gerstenschläger *et al.* (1993).

NPL4 Encodes a Protein that Is Located at the Nuclear Periphery

The *NPL4* sequence is predicted to encode a protein of 580 amino acids (63.8 kDa) and contains several highly degenerate repeats, including GSXS, GSSX, GSXF, and GFXS, which are found in Nup214p/CANp (von Lindern *et al.*, 1992; Kraemer *et al.*, 1994), Nup159p/Rat7p (Gorsch *et al.*, 1995), Nup100p (Wente *et al.*,

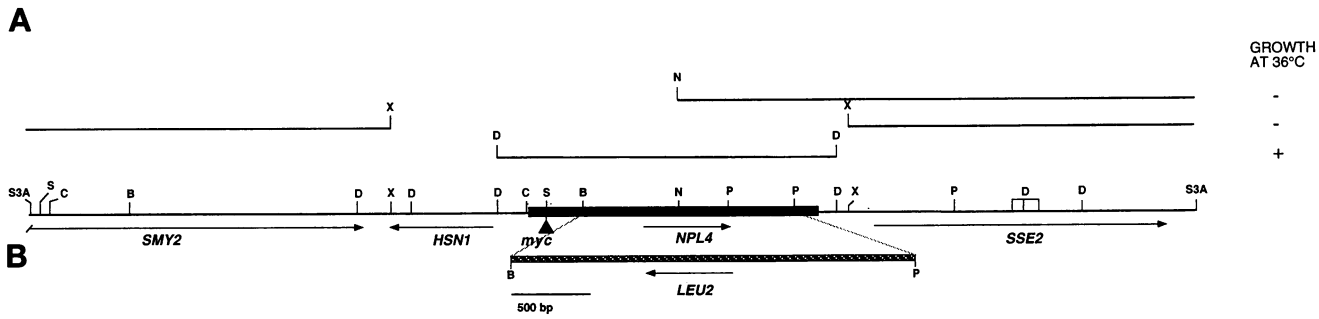

C

```
MLIRFRSKNGTHRVSCQENDLFGTVIEKLVGNLDPNADVDTFTVCEKPGQ 50
GIHAVSELADRTVMDLGLKHDDMLILNYSDKPANEKDGVNVEIGSVGIDS100
KGIRQHRYGPLRIKELAVDEELEKEDGLIPRQKSKLCKHGDRGMCEYCSP150
LPPWDKEYHEKNKIKHISFHSYLKKLNENANKKENGSSYSPLSEPDFRI 200
NKRCHNGHEPWPRGICSKCQPSAITLQQQEFRMVDHVEFQKSEIINEFIQ 250
AWRYTGMQRFGYMYGSYSKYDNTPLGIKAVVEAIYEPPQHDEQDGLTMDV 300
EQVKNEMLQIDRQAQEMGLSRIGLIFTDLSDAGAGDGSVFCKRHKDSFFL 350
SSLEVIMAARHQTRHPNVSKYSEQGFFSSKFVTCVISGNLEGEIDISSYQ 400
VSTEAEALVTADMISGSTFPSMAYINDTTDERYVPEIFYMKSNEYGITVK 450
ENAKPAFPVDYLLVTLTHGFPNTDTETNSKFVSSTGFPWSNRQAMGQSQD 500
YQELKKYLFNVASSGDFNLLHEKISNFHLLLYINSLQILSPDEWKLLIES 550
AVKNEWEESLLKLVSSAGWQTLVMILQESG 580
```

Figure 1. The *NPL4* coding region. (A) The minimal complementing region of the *NPL4* clone. The lines above the map represent fragments of the cloned DNA tested for complementation of the *npl4-1* Ts^- defect. The column at the right indicates the results of these tests. (B) The *NPL4* gene replacement and myc tagging. The *Bam*HI-*Pst*I fragment of *NPL4* was removed and replaced by a *Bam*HI-*Pst*I fragment of *LEU2*. The *NPL4 Sal*I site was inserted with a c-myc epitope. (A and B) B, *Bam*HI; C, *Cla*I; D, *Dra*I; E, *Eco*RI; P, *Pst*I; S, *Sal*I; S3A, *Sau*3AI; X, *Xba*I. (C) The sequence of Np14p. The XXFG and other degenerate repeats are in bold and italicized. The serine doublets are in bold. The sequence data are available from GenBank under accession number X72224.

1992), Nup153p (Sukegawa and Blobel, 1993), Nup358p (Wu *et al.*, 1995; Yokoyama *et al.*, 1995), Pom121p (Hallberg *et al.*, 1993), and other NPC proteins. The GSXS, GSSX, GSXF, and GFXS repeats occur in Nup214p/CANp and other NPC proteins at or near the previously described XXFG, GLFG, or XFXFG repeats. It should be noted that Nup214p/CANp contains 21 total GSXS, GSSX, GSXF, and GFXS repeats, whereas Npl4p contains six total repeats. Moreover, most of the Nup214p/CANp GSXS, GSSX, GSXF, and GFXS repeats are located in the C-terminal domain of the protein, whereas the Npl4p repeats are distributed throughout the protein. In addition, Npl4p contains two XXFG repeats (Figure 1B) and seven serine doublets (Figure 1B), whereas Nup214p/CANp contains 17 XXFG repeats and 39 serine runs (Kraemer *et al.*, 1994).

We generated affinity-purified antibodies to Npl4p (see MATERIALS AND METHODS) and used these antibodies to probe cell extracts prepared from wild-type cells (Figure 2A, lane 1) and cells transformed with single-copy (Figure 2A, lane 2), high-copy (Figure 2A, lane 3), and *GAL1* promoter-*NPL4* (Figure 2A, lane 4)-containing plasmids (see MATERIALS AND METHODS). The anti-Npl4p antibodies specifically recognize a protein band that migrates at ~69 kDa, ~5 kDa larger than the predicted molecular mass of Npl4p. We noted that cells carrying the high-copy

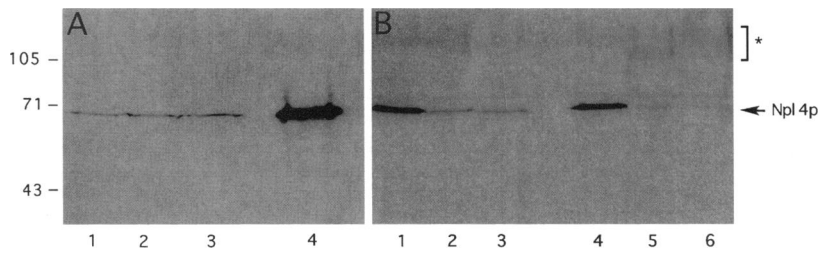

Figure 2. (A) Immunoblotting demonstrates that the anti-Npl4p antibody specifically recognizes Npl4p. Whole-cell extracts from wild-type cells (lane 1) and wild-type cells carrying single-copy (lane 2), high-copy (lane 3), and galactose-induced (lane 4) *NPL4*-containing plasmids were probed with affinity-purified antibodies generated against Npl4p. (B) *Npl4* cells have decreased levels of Npl4p. Whole-cell extracts were prepared from wild-type, *npl4-1*, and *npl4-2* cells maintained at RT (lanes 1–3) or shifted to 37°C for 5 h (lanes 4–6) and probed with anti-Npl4 antibodies.

NPL4 plasmid show only a ~twofold increase in Npl4p levels compared with wild-type cells. Comparable results have been observed for *RNA14* and *RNA15* (Bonneaud *et al.*, 1994).

To investigate whether the *npl4-1* and *npl4-2* mutations affect the levels of Npl4p, we performed immunoblot analysis of the *npl4* mutants. Wild-type, *npl4-1*, and *npl4-2* cells were grown at RT or shifted to 37°C for 5 h, used to prepare cell extracts, and probed with the anti-Npl4p antibody (see MATERIALS AND METHODS). At the permissive temperature, *npl4-1* cell extracts have a ~fourfold decrease in Npl4p (Figure 2B, lane 2), and *npl4-2* cell extracts have a ~fivefold decrease in Npl4p (Figure 2B, lane 3) compared with wild-type cells (Figure 2B, lane 1). After a shift to the nonpermissive temperature, *npl4-1* cell extracts have a ~7-fold decrease in Npl4p (Figure 2B, lane 5), whereas *npl4-2* cell extracts have a ~29-fold decrease in Npl4p (Figure 2B, lane 6). These results indicate that *npl4-2* cells have lower levels of Npl4p than *npl4-1* cells, and this difference increases at the nonpermissive temperature. We noted that the *npl4* extracts are distinguished by several cross-reacting bands, which run ~100-200 kDa (Figure 2B, lanes 5 and 6). These bands may represent Npl4p multimers or aggregates. In *npl4-2* cell extracts, the bands appeared after a 1-h temperature shift, whereas in *npl4-1* extracts, they appeared after a 2-h temperature shift (our unpublished observations). Thus, *npl4-2* cells may have more rapid oligomerization or aggregation of Npl4p at the nonpermissive temperature.

To determine the intracellular location of Npl4p, we incubated wild-type diploid cells with the anti-Npl4p antibody and examined the cells by indirect immunofluorescence (IF; see MATERIALS AND METHODS). The cells show punctate, rim staining of the nucleus (Figure 3A), suggesting localization to the NPC. Similar staining is seen in Δ*npl4* cells rescued with plasmid encoding a Npl4-myc protein and incubated with anti-myc antibodies (our unpublished results), indicating that the anti-Npl4p antibody specifically recognizes Npl4p at the yeast nuclear envelope. Moreover, Npl4p localizes in a pattern similar to a known NPC protein; wild-type diploid cells incubated with both anti-Npl4p and anti-Nup159p/Rat7p antibodies show comparable staining patterns (Figure 3, D and E). In addition, Npl4p is mislocalized in *rat3-1* cells in a pattern consistent with NPC clustering previously observed in this mutant (Figure 3, G and H). The sum of these observations suggests that Npl4p is a nucleoporin or a NPC-associated protein. It should be noted that the Npl4p signal is weaker than the Nup159p/Rat7p signal and is absent in several *rat3-1* cells. It is possible that Npl4p is less accessible than Nup159p/Rat7p; Npl4p antibody recognition is extremely sensitive to formaldehyde fixation, whereas Nup159p/Rat7p antibody recognition is not. Additionally, anti-Npl4p staining requires significantly higher antibody concentrations than anti-Nup159p/Rat7p staining. In the *rat3-1* cells, NPC clustering may further reduce Npl4p antibody recognition.

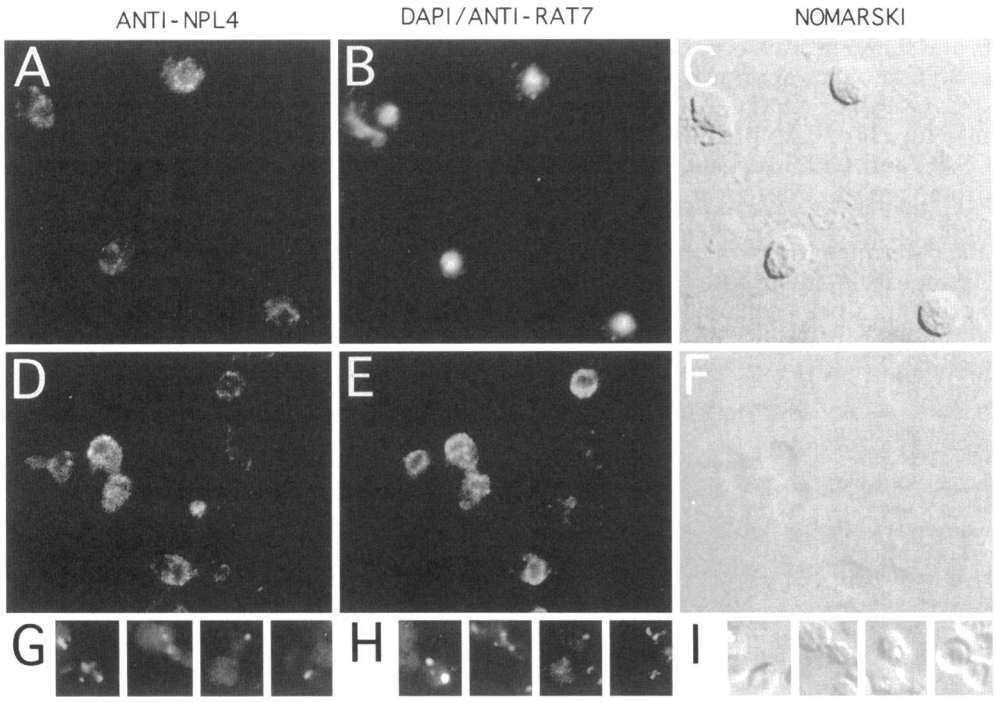

Figure 3. Immunolocalization of Npl4p to the yeast nuclear envelope. Wild-type diploid cells were incubated with anti-Npl4p antibodies (A–C) or wild-type diploid (D–F), and *rat3-1* haploid (G–I) cells were coincubated with anti-Npl4p and anti-Nup159p/Rat7p antibodies and prepared for indirect immunofluorescence. (A) The anti-Npl4p staining pattern; (B) the same cells stained with DAPI, and (C) viewed using Nomarksi optics; (D and G) the anti-Npl4p staining pattern; (E and H) the same cells stained with anti-Nup159p/Rat7p, and (F and I) viewed using Nomarski optics.

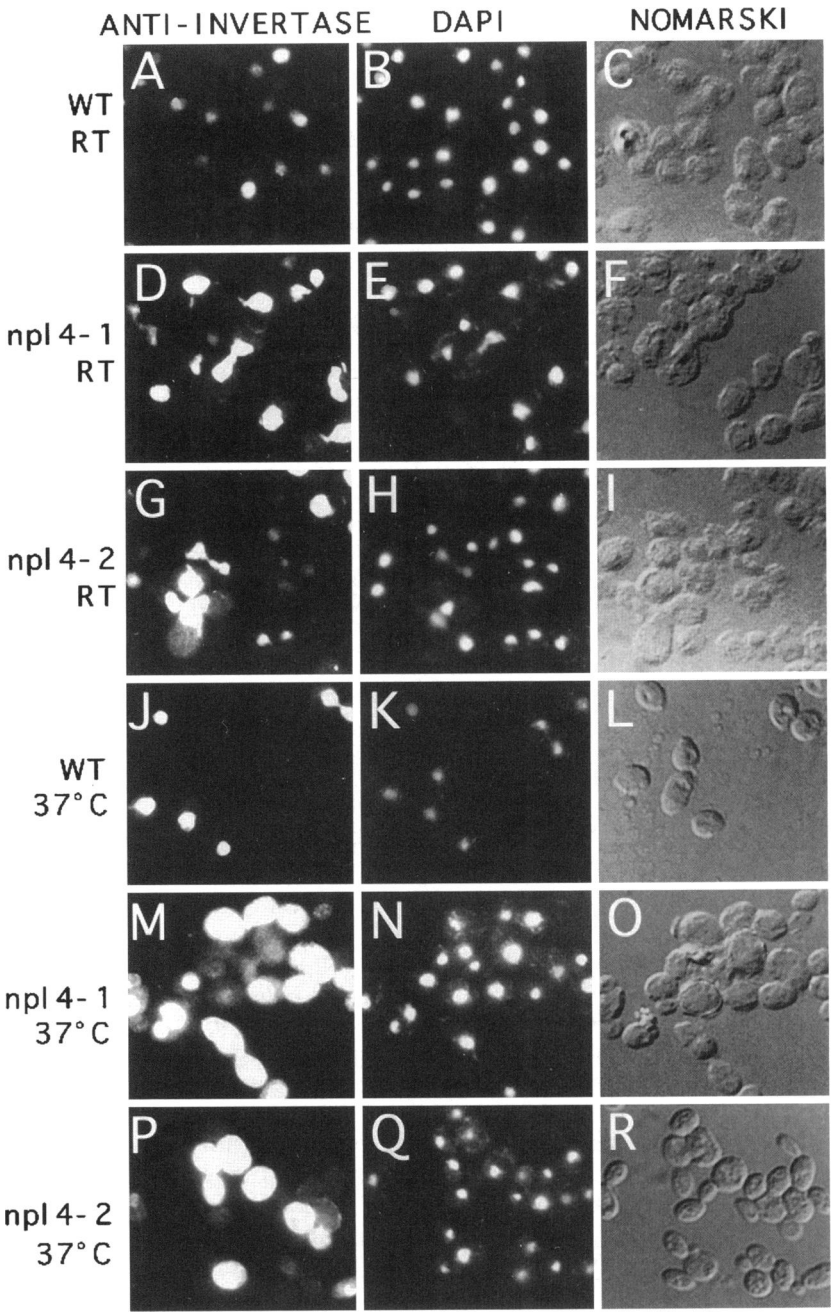

Figure 4. *Npl4* cells mislocalize of the NLS-invertase reporter protein at the nonpermissive temperature. Wild-type, *npl4-1*, and *npl4-2* cells expressing the fusion protein were maintained at RT (A–C, D–F, and G–I) or shifted to 37°C for 3 h (J–L, M–O, and P–R), incubated with anti-invertase, and prepared for indirect immunofluorescence. (A, D, G, J, M, and P) The anti-invertase staining pattern; (B, E, H, K, N, and Q) the same fields stained with DAPI; and (C, F, I, L, O, and R) and viewed using Nomarski optics.

npl4-1 and npl4-2 Cells Are Defective for Nuclear Protein Import

Cells that have defective NPC proteins can have nuclear protein import defects (reviewed in Doye and Hurt, 1995). Since Npl4p localizes in a pattern similar to NPC proteins and *npl4-1* cells mislocalize endogenous nuclear proteins (Bossie *et al.*, 1992), we tested *npl4* cells for additional defects in nuclear protein import in vivo. Wild-type and *npl4* cells were transformed with a reporter construct containing the *GAL1* promoter and the SV40 NLS fused to invertase (NLS-invertase). Transformants were grown at RT in selective media, the fusion protein was induced for 3 h by the addition of galactose, and cells were grown at RT or shifted to 37°C for 30 min or 3 h and examined by IF (see MATERIALS AND METHODS). At RT and after 30 min (our unpublished results) or 3 h (Figure 4, A and J) at 37°C, wild-type cells localize the NLS-invertase exclusively to the nucleus. At RT, 0% of the *npl4-1* cells and ~3% of the *npl4-2* cells accumulate

small amounts of NLS-invertase in the cytoplasm (Figure 4G). After 30 min at 37°C, ~0.1% of the *npl4-1* cells and ~39% of the *npl4-2* cells accumulate significant amounts of NLS-invertase in the cytoplasm (our unpublished results). After 3 h at 37°C, ~48% of the *npl4-1* cells and ~42% of the *npl4-2* cells accumulate significant amounts of NLS-invertase in the cytoplasm (Figure 4, M and P). It was noted that approximately one-half of *npl4* cells show cytoplasmic accumulation of NLS-invertase after a 3-h temperature shift and that the level of NLS-invertase staining varies from cell to cell. We reasoned that this is due to differences in the levels of the fusion protein in individual cells, since ~60% of the wild-type cells show nuclear staining with NLS-invertase, and the intensity of nuclear staining also varies from cell to cell. Similar results were obtained using a reporter construct containing the *GAL1* promoter and the H2B NLS fused to β-galactosidase (NLS-β-galactosidase; Moreland *et al.*, 1987; our unpublished observations). It was also noted that the *npl4* nuclei appear to be enlarged relative to the wild type; this was confirmed by electron microscopy (see below).

To rule out the possibility that the cytoplasmic accumulation of nuclear proteins was due to proteins "leaking" out of the nucleus, the *npl4* cells were assayed for nuclear protein retention. Wild-type and *npl4* cells were transformed as described above and grown at RT in selective media. The fusion protein was induced for 3 h by the addition of galactose and repressed for 1.5 h in glucose; the cells were grown at RT or shifted to 37°C for 3 h and examined by IF (see MATERIALS AND METHODS). At RT and 37°C, both wild-type and *npl4* cells successfully maintained the NLS-invertase and the NLS-β-galactosidase fusion proteins inside the nucleus (our unpublished results). In contrast, previous experiments have shown that *sec63-1* cells fail to retain NLS-invertase fusion protein inside the nucleus at the nonpermissive temperature (Chiang, 1993). These results indicate that the *npl4* nuclear protein localization defects are due to an inability to import nuclear proteins, not an inability to retain proteins inside the nucleus.

To examine the nuclear protein import defect of the *npl4* cells more directly, we tested the mutants in a yeast in vitro import assay (Schlenstedt *et al.*, 1993). The in vitro assay uses semi-intact cells added to exogenous cytosol, an energy-regenerating system, and an exogenous, fluorescently labeled SV40-NLS-HSA import substrate (Schlenstedt *et al.*, 1993). With the addition of cytosol and energy, the import substrate accumulates inside the cell nucleus, but in the absence of cytosol and/or energy, the substrate binds at the nuclear rim (Schlenstedt *et al.*, 1993). In vitro nuclear import has been shown to duplicate all of the requirements of nuclear protein import and has been used to demonstrate nuclear import defects for cells with defective NPC proteins (Schlenstedt *et al.*, 1993). Notably, the in vitro assay avoids the complications inherent in the in vivo assays, since the added import substrate precludes any requirements for RNA export and protein synthesis.

For the in vitro assay, wild-type and *npl4* cells were grown at RT or shifted to 37°C for 3 h, used to prepare cytosol and semi-intact cells, added to energy and substrate mixtures, and examined by fluorescence microscopy (see MATERIALS AND METHODS). Approximately 37% of semi-intact cells prepared from wild-type cells shifted to 37°C show nuclear accumulation of substrate when incubated with cytosol prepared from wild-type cells grown at 37°C (Figure 5) or RT (Figure 6A). Similarly, 32–35% of semi-intact cells prepared from wild-type cells shifted to 37°C show nuclear accumulation of substrate when incubated with cytosol prepared from *npl4* cells grown at 37°C (Figure 5) or RT (our unpublished results). In contrast, 0–4% of semi-intact cells prepared from *npl4* cells shifted to 37°C accumulate substrate in the nucleus when incubated with cytosol prepared from wild-type cells grown at 37°C (Figure 5) or RT (Figure 6, D and G). This defect in nuclear accumulation is not observed in semi-intact cells prepared from *npl4* cells grown at RT (our unpublished results) and is not attributable to differences in the permeability of

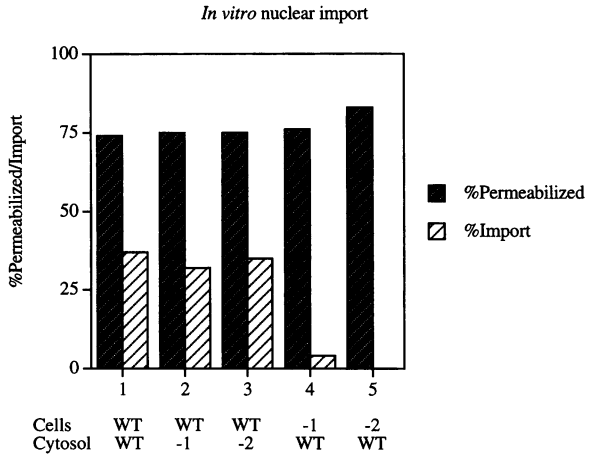

Figure 5. *Npl4* cytosol supports the import of NLS-HSA substrate at the nonpermissive temperature. Wild-type, *npl14-1*, and *npl4-2* cells were shifted to 37°C and used to prepare semi-intact cells. Semi-intact cells were added to cytosol prepared from wild-type or *npl4* cells shifted to 37°C, import substrate, energy-regenerating system, stained with DAPI, and viewed by fluorescence microscopy. Permeability and import levels were determined as described (see MATERIALS AND METHODS). WT, wild-type cells or cytosol; −1, *npl4-1* cells or cytosol; −2, *npl4-2* cells or cytosol. The results are representative of observed import reactions.

wild-type and *npl4* semi-intact cells (Figure 5). These results confirm that *npl4* cells have Ts^- defects for nuclear import and indicate that these defects are conferred by nuclear components. We noted that certain temperature-shifted semi-intact *npl4-1* cells are marked by small spots of substrate (Figure 6D). It is possible that these spots represent small amounts of substrate binding, because they appear at the nuclear rim and are present even the in absence of cytosol (our unpublished observations). Alternately, these spots may represent nonspecific aggregation of import substrate.

npl4-2 Cells Retain Poly(A)$^+$ RNA in the Nucleus

Since cells with defective NPC proteins can have RNA export defects (Doye and Hurt, 1995), we assayed *npl4* poly(A)$^+$ RNA export by in situ hybridization (Amberg *et al.*, 1992). Wild-type and *npl4* cells were grown at RT or shifted to 37°C for 30 min and incubated in the presence or absence of oligo(dT)$_{50}$ digoxigenin-labeled probe and examined by IF (see MATERIALS AND METHODS). At RT, oligo(dT)$_{50}$ probe is hybridized in the cytoplasm of wild-type and *npl4* cells (Figure 7, A, D, and G), consistent with efficient poly(A)$^+$ RNA export. At 37°C, oligo(dT)$_{50}$ probe is still hybridized in the cytoplasm of wild-type and *npl4-1* cells (Figure 7, J and M). In *npl4-2* cells, the oligo(dT)$_{50}$ probe is hybridized in a ring-like pattern at the nucleus (Figure 7P). These results suggest that *npl4-2* cells have a block in poly(A)$^+$ RNA export and that poly(A)$^+$ RNA accumulates at the *npl4-2* nuclear periphery. We noted that *npl4* cells, which appeared normal for poly(A)$^+$ RNA export, hybridized more oligo(dT)$_{50}$ in the cytoplasm than wild-type cells (Figure 7, D, G, and M); this has been observed for other *nup* mutants (Davis, personal communication).

Nuclear Envelope in npl4-1 and npl4-2 Cells

Cells with defective NPC proteins can have alterations in nuclear structure (Doye and Hurt, 1995). We, therefore, examined the *npl4* cells by electron microscopy. Wild-type and *npl4* cells were grown at RT or shifted to 37°C for 30 min, 3 h, or 5 h, used to prepare thin sections, and analyzed by TEM (see MATERIALS AND METHODS). At RT, *npl4-1* (Figure 8B) and *npl4-2* (Figure 8C) cells are similar to wild-type cells (Figure 8A). At 37°C, *npl4-1* cells are ~1.1-fold larger than wild-type cells, contain nuclei that are ~1.4-fold larger than wild-type cells, and are filled with membrane projections extending from the nuclear envelope into the cytoplasm (Figure 8E, arrow). Similarly, *npl4-2* cells are ~1.8-fold larger than wild-type cells and contain nuclei that are ~3-fold larger than wild-type cells, but these cells are marked by multiple

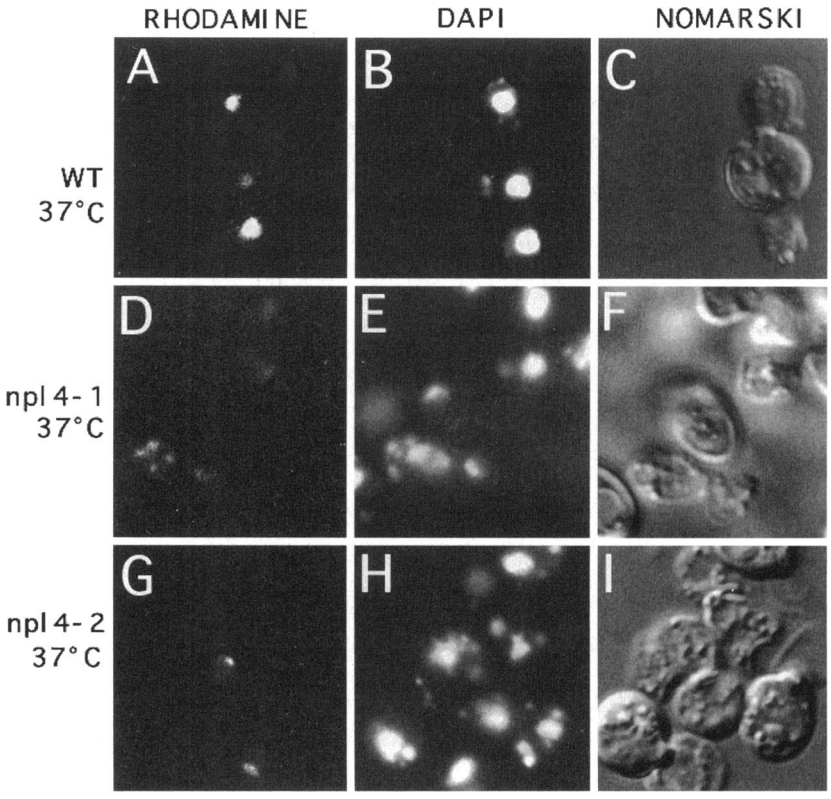

Figure 6. Npl4 semi-intact cells fail to import NLS-HSA substrate at the nonpermissive temperature. Wild-type (A–C), *npl4-1* (D–F), and *npl4-2* (G–I) cells were shifted to 37°C for 3 h and used to prepare semi-intact cells. Semi-intact cells were added to cytosol prepared from wild-type cells grown at RT, import substrate, energy-regenerating system, stained with DAPI, and viewed by fluorescence microscopy. (A, D, and G) The NLS-HSA fluorescent substrate staining pattern; (B, E, and H) the same fields stained with DAPI; and (C, F, and I) and viewed using Nomarski optics.

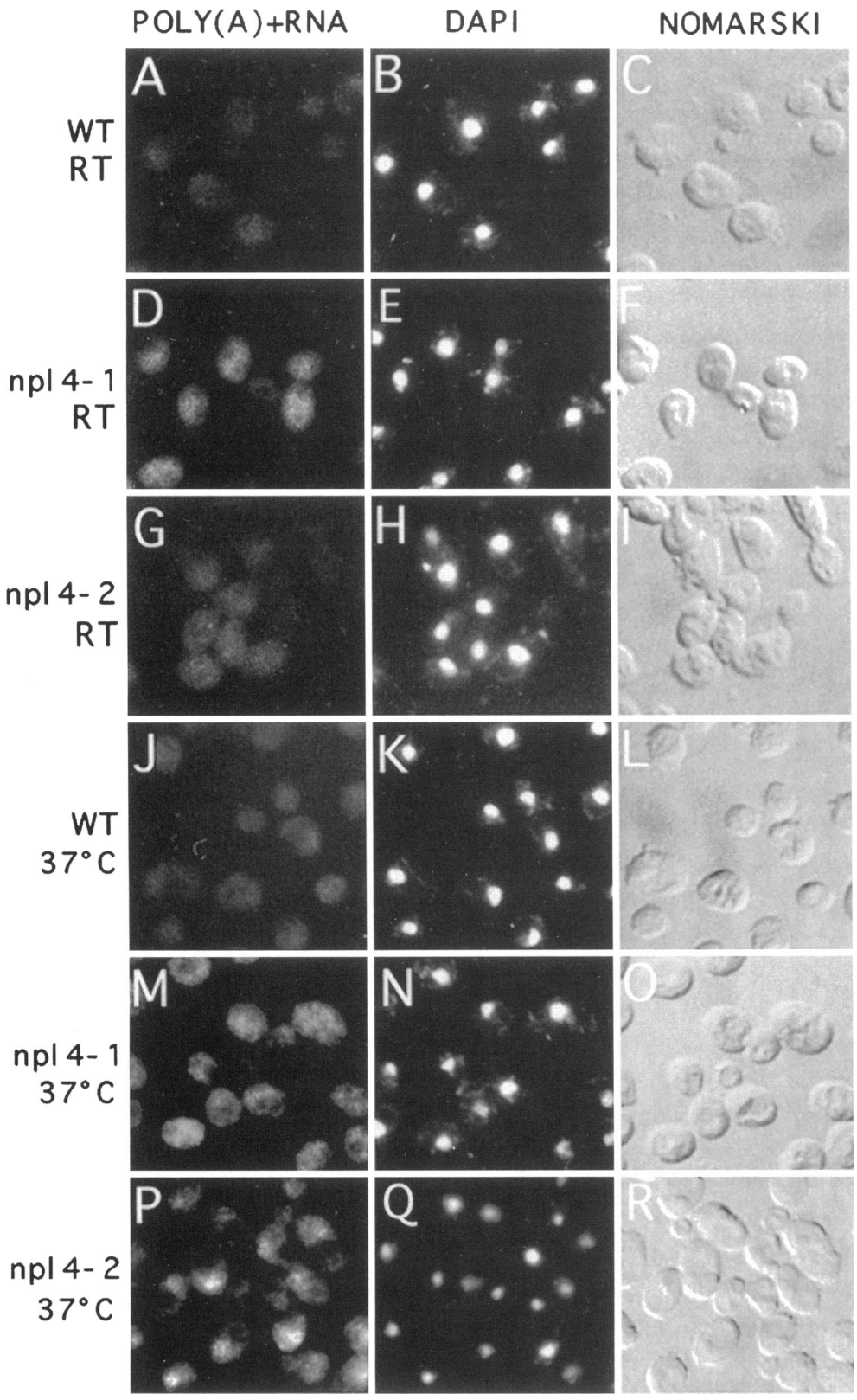

Figure 7. *Npl4-2* cells mislocalize poly(A)$^+$ RNA at the nonpermissive temperature. Wild-type, *npl4-1*, and *npl4-2* cells were grown at RT (A–C, D–F, and G–I) or shifted to 37°C for 30 min (J–L, M–O, and P–R), incubated with oligo(dT)$_{50}$-digoxigenin probe, and prepared for indirect immunofluorescence. (A, D, G, J, M, and P) The oligo(dT)$_{50}$-digoxigenin probe localization pattern: (B, E, H, K, N, and Q) the same fields stained with DAPI; and (C, F, I, L, O, and R) and viewed using Nomarski optics.

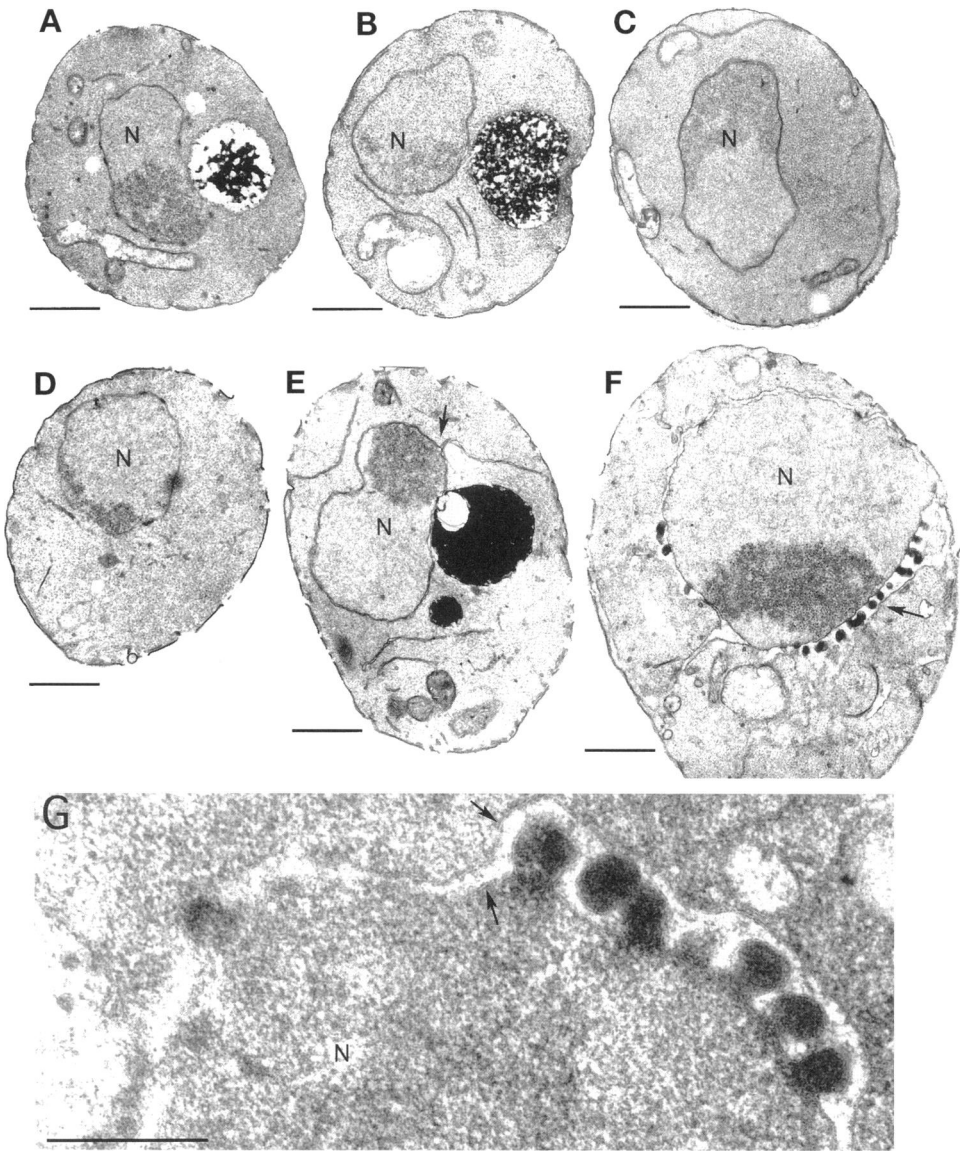

Figure 8. *Npl4* cells exhibit altered nuclear envelope structure at the nonpermissive temperature. Electron micrographs of wild-type, *npl4-1*, and *npl4-2* cells grown at RT (A–C) or shifted to 37°C for 5 h (D–F) and prepared for TEM. Arrows denote *npl4-1* nuclear envelope projections (E), *npl4-2* nuclear envelope herniations (F), and *npl4-2* inner and outer nuclear membranes (G). (A–F) Bars, 1 μm; (G) bar, 0.2 μm.

nuclear envelope herniations that are filled with electron-dense material (Figure 8F, arrow). Notably, the *npl4-2* herniations distend both the inner and outer nuclear membranes (Figure 8G, arrows) and tend to appear on one side of the nuclear envelope. This phenotype is strikingly similar to the one observed for Δ*nup116* cells (Wente and Blobel, 1993). For *npl4-1*, 0, ~78, or ~91% of the cells exhibit significant nuclear envelope projections after 30-min, 3-h, or 5-h shifts to 37°C. For *npl4-2*, ~7,~67, or ~90 of the cells exhibit nuclear envelope herniations after 30-min, 3-h, or 5-h shifts to 37°C. In addition, the *npl4-2* cells exhibiting nuclear envelope herniations show ~1, ~5, and ~13 herniations per nucleus after 30-min, 3-h, or 5-h temperature shifts. Thus, *npl4* cells have distinct nuclear envelope defects that become increasingly pronounced at the nonpermissive temperature. We noted that NPCs were more difficult to detect in the *npl4* micrographs. This may be due to the staining technique, which preferentially visualizes the nuclear envelope, and staining differences between wild-type cells and *npl4* NPCs.

To ensure that the *npl4-1*and *npl4-2* morphological differences were due to different mutations in *NPL4*, we constructed isogenic mutant strains and examined these strains by electron microscopy. The *npl4-1* and *npl4-2* mutations were cloned using the plasmid gap-repair method, the plasmids were checked for the Ts^- mutations, and used to rescue the Δ*npl4* haploid strain (see MATERIALS AND

METHODS). Δ*Npl4* cells rescued with single-copy plasmids containing wild-type *NPL4*, *npl4-1*, or *npl4-2* were grown for 5 h at 37°C, used to prepare thin sections, and examined by TEM (see MATERIALS AND METHODS). The Δ*npl4* cells rescued with the wild-type *NPL4* plasmid appear to be normal (Figure 9A), whereas Δ*npl4* cells carrying the *npl4-1* plasmid (Figure 9B) and the *npl4-2* plasmid (Figure 9C) have structural differences comparable to the original *npl4-1* and *npl4-2* strains. This indicates that the distinctive nuclear structures exhibited by *npl4-1* and *npl4-2* cells are caused by different mutations in *NPL4*. We observed some variations between the isogenic and original *npl4* strains. For isogenic *npl4-1*, only ~18% of the cells exhibit nuclear membrane projections after a 5-h shift to the nonpermissive temperature. For isogenic *npl4-2*, ~78% of the cells exhibit nuclear envelope herniations after a 5-h shift to the nonpermissive temperature, but the herniations are not neatly arrayed in the nuclear envelope (compare Figs. 8G and 9C). Since these disparities were observed under identical growth conditions, they were attributed to the different genetic backgrounds of the original and isogenic strains.

Since Δ*nup116* NPCs were localized to the base of nuclear envelope herniations (Wente and Blobel, 1993), we determined the localization of *npl4-2* NPCs by immunoelectron microscopy. *Npl4-2* cells were grown at 37°C for 5 h and used to make frozen thin sections, which were incubated with the polyspecific NPC MAb414 (Aris and Blobel, 1989), and examined by TEM (see MATERIALS AND METHODS). In *npl4-2* cells, gold particles were specifically localized to the inner nuclear membrane and the base of nuclear envelope herniations (Figure 10, A and B), at concentrations of ~21 particles/μm^2. In contrast, gold particles were distributed nonspecifically in the nucleoplasm and cytoplasm of *npl4-2* cells at concentrations of ~1 particle/μm^2. Virtually no gold particles were associated with the interior compartment or exterior surface of the nuclear envelope herniations. These results indicate that *npl4-2* MAb414-reactive NPC proteins are located at the at the foot of nuclear envelope herniations and are consistent with the results for Δ*nup116* (Wente and Blobel, 1993).

To investigate whether the *npl4-2* nuclear envelope herniations were filled with the poly(A)$^+$ RNA that appeared to accumulate at the nuclear periphery (see Figure 8P), we localized poly(A)$^+$ RNA by TEM (Huang *et al.*, 1994). Wild-type and *npl4-2* cells were grown at RT, shifted to 37°C for 3 h, incubated with or without oligo(dT)$_{50}$ probe, and viewed by TEM (see MATERIALS AND METHODS). In the presence of oligo(dT)$_{50}$ probe, wild-type cells are decorated with numerous gold particles in the nucleus and cytoplasm (Figure 11A), whereas the *npl4-2* cells are decorated with several gold particles at nuclear protrusions (Figure 11C). In the absence of oligo(dT)$_{50}$ probe, gold particles are not seen in wild-type or *npl4-2* cells (Figure 11, B and D). These results, the results of our poly(A)$^+$ RNA assay, and our ultrastructural observations, suggest that *npl4-2* cells accumulate poly(A)$^+$ RNA to form herniations at the nonpermissive temperature. It should be noted that the TEM in situ hybridization procedure disrupts the *npl4-2* membranes and prevents de-

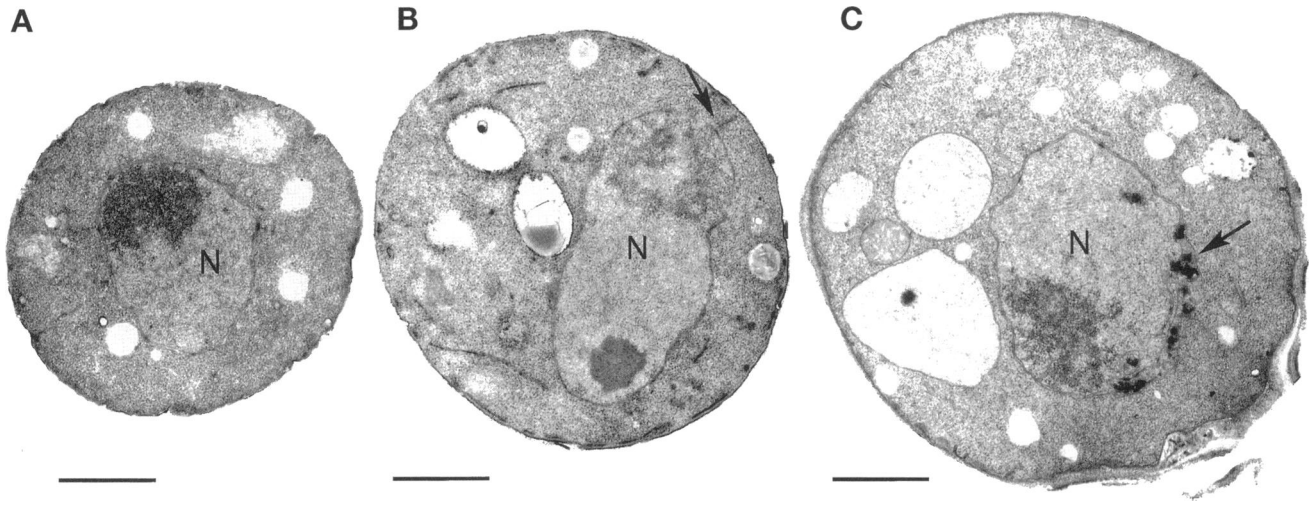

Figure 9. Isogenic *npl4-1* and *npl4-2* strains exhibit nuclear structural defects at the nonpermissive temperature. Electron micrographs of Δ*npl4* cells rescued by wild-type *NPL4*- (A), *npl4-1*- (B), and *npl4-2*- (C) containing plasmids and shifted to 37°C for 5 h and prepared for TEM. (A, B, and C) Bars, 1 μm.

tailed analysis of the nuclear envelope structure; this has been observed in previous studies (Tani *et al.*, 1995). In addition, the nuclear protrusions were decorated with only ~3 gold particles per protrusion (Figure 11C). We hypothesize that the *npl4-2* herniations are filled with poly(A)$^+$ RNA and other export materials which are too tightly packed to allow efficient hybridization of the oligo(dT)$_{50}$ probe.

Both *npl4-2* and Δ*nup116* cells exhibit nuclear envelope herniations at the nonpermissive temperature, suggesting that Npl4p and Nup116p have overlapping functions. To test this idea, we checked high-copy plasmids carrying *NPL4* and *NUP116* plasmids for the ability to rescue the Δ*nup116* and *npl4-1*/*npl4-2* Ts$^-$ defects, respectively (see MATERIALS AND METHODS). Plasmids carrying high-copy *NUP116* were unable to rescue the *npl4-1* or *npl4-2* Ts$^-$ defect (our unpublished observations). In contrast, a high-copy plasmid containing *URA3* and *NPL4* was able to partly rescue the Δ*nup116* Ts$^-$ defect (Figure 12B, section 3), and a plasmid containing *URA3* and the *GAL1* promoter and *NPL4* was able to weakly rescue the Δ*nup116* Ts$^-$ defect in the presence of galactose (Figure 12D, section 4). This rescue was not observed for Δ*nup116* strains transformed with a plasmid carrying single-copy *NPL4* (Figure 12B, section 2) or vector alone (Figure 12B, section 1). Moreover, the Δ*nup116* strains transformed with high-copy *NPL4* or *GAL1* promoter-*NPL4* were unable to grow on 5-FOA at 36°C (Figure 12F, sections 3 and 4), indicating that the cells were unable to lose the *NPL4*-containing plasmid at the nonpermissive temperature. The sum of these results suggest that Npl4p can partly substitute for Nup116p in the cell, but Nup116p cannot substitute for Npl4p. This is consistent with the observation that the *NPL4* gene is essential, whereas the *NUP116* gene is required for growth only at the restrictive temperature (Wente and Blobel, 1993). We noted that Δ*nup116* cells carrying a single-copy *NUP116* plasmid showed significant growth within 24 h at 36°C, whereas Δ*nup116* cells carrying a high-copy *NPL4* plasmid showed significant growth after 48 h at 36°C. In addition, we observed that plasmids containing *GAL1* promoter-*NPL4* weakly rescue the Δ*nup116* Ts$^-$ defect in the presence of glucose and galactose (Figure 12D, section 4) and fail to rescue the Δ*nup116* Ts$^-$ defect in the presence of galactose alone (our unpublished observations). These results imply that the high-copy *NPL4* plasmid rescue of the Δ*nup116* Ts$^-$ defect is delayed and dose dependent.

Since a high-copy plasmid containing *NPL4* partly rescues the Δ*nup116* growth defect, we investigated whether the *NPL4* plasmid could partly correct the Δ*nup116* structural defects. Δ*Nup116* cells carrying a single-copy *NUP116* plasmid, a high-copy *NPL4* plasmid, or vector alone were grown in selective media, shifted to 34°C for 5 h, used to prepare thin sections, and examined by TEM (see MATERIALS AND METHODS). We noted that the lower temperature (34°C) facilitated the growth of Δ*nup116* cells carrying a high-copy *NPL4* plasmid in liquid media, but restricted the growth of Δ*nup116* cells carrying vector alone (our unpublished observations). For Δ*nup116* cells carrying the single-copy *NUP116* plasmid, ~1% of the cells show nuclear envelope herniations, and these cells exhibit ~3 herniations per nucleus. For Δ*nup116* cells carrying vector alone, all of the cells show nuclear envelope herniations, and ~80% of these cells exhibit ≥5 herniations per nucleus. For Δ*nup116* cells carrying the high-copy *NPL4* plasmid, all of the cells showed nuclear envelope herniations, but only ~40% of these cells showed ≥5 herniations per nucleus. These results indicate that the high-copy *NPL4* plasmid can mitigate the severity of the Δ*nup116* structural defects.

DISCUSSION

We previously identified *npl4-1* as a yeast mutant defective in nuclear protein localization using a modified genetic screen (Bossie *et al.*, 1992). Presently, we describe the *npl4-1* and *npl4-2* defects in nuclear function and structure using a number of different assays. *Npl4* cells exhibit temperature-sensitive defects for in vivo and in vitro nuclear protein import, and *npl4-2* cells exhibit a temperature-sensitive defect for poly(A)$^+$ RNA export. In addition, *npl4* cells display temperature-sensitive alterations in nuclear structure; *npl4-1* cells produce nuclear envelope projections and *npl4-2* cells create nuclear envelope herniations which

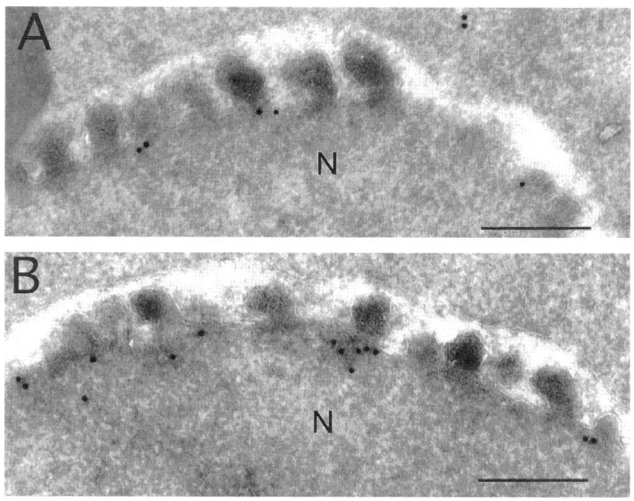

Figure 10. *Npl4-2* NPCs are localized to the base of nuclear envelope herniations. Electron micrographs of *npl4-2* cells shifted to 37°C for 5 h and prepared for immunolocalization with MAb414. (A and B) The panels depicted are representative of observed micrographs. (A and B) Bars, 0.125 μm.

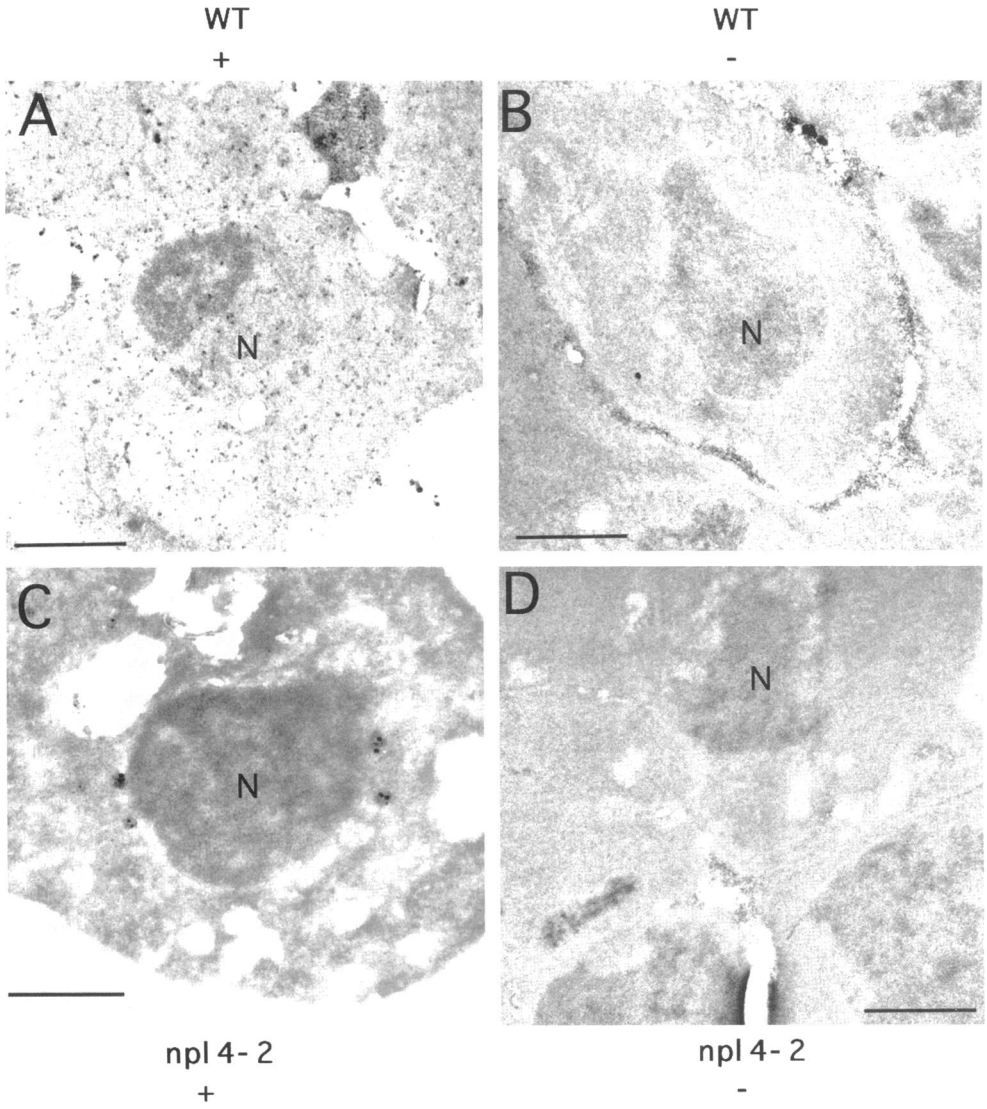

Figure 11. *Npl4-2* cells accumulate poly(A)$^+$ RNA inside nuclear protrusions. Electron micrographs of wild-type (A and B) and *npl4-2* (C and D) cells shifted to 37°C for 3 h, incubated in the presence (A and C) or absence (B and D) of oligo(dT)$_{50}$-digoxigenin probe, and prepared for in situ hybridization-TEM. WT, wild type. (A, B, and D) Bars, 1 μm; (C) bar, 0.5 μm.

encapsulate poly(A)$^+$ RNA. These defects are consistent with the observations that the Npl4p is localized at the nuclear rim, similar to known NPC proteins.

The sequence of *NPL4* predicts a protein with highly degenerate repeats that are found in Nup214p/CANp and other NPC proteins. It is thought that NPC protein repeat motifs represent multiple modular structural regions and multiple separable functions of nucleoporins or sites of interaction with nuclear transport factors/substrates (Rout and Wente, 1994). The GLFG repeat domain of vertebrate Nup98p provides docking activity for NLS-HSA import substrate in vitro (Radu *et al.*, 1995b), the Nup1p and Nup2p FXFG repeat sequences bind to Kap60p-Kap95p heterodimers in vitro (Rexach and Blobel, 1995), and the Nup116p GLFG repeat sequences bind to Kap95p in in vitro and yeast two-hybrid assays (Iovine *et al.*, 1995). In addition, the Nup100p and Nup159p XXFG repeat sequences bind to the HIV-1 Rev protein in yeast two-hybrid assays (Stutz *et al.*, 1995), and the FG repeat regions of hRIPp, Nup153p, Nup98p, POM121p, Nup159p, and Nup214p/CANp bind to the nuclear export sequence regions of HIV-1 Rev, HTLV-1 Rex, PKI, and IFκB in yeast two-hybrid assays (Fritz and Green, 1996). It is not known whether the GSXS, GSSX, GSXF, and GFXS repeats in Npl4p and Nup214p/CANp have structural and/or functional significance. It was noted that Nup214p/CANp has more repeats than Npl4p and that Nup214p/CANp concentrates these repeats in its C-terminal domain. At this time, we cannot speculate on the differences in the frequency and distribution of GSXS, GSSX, GSXF, and GFXS repeat sequences.

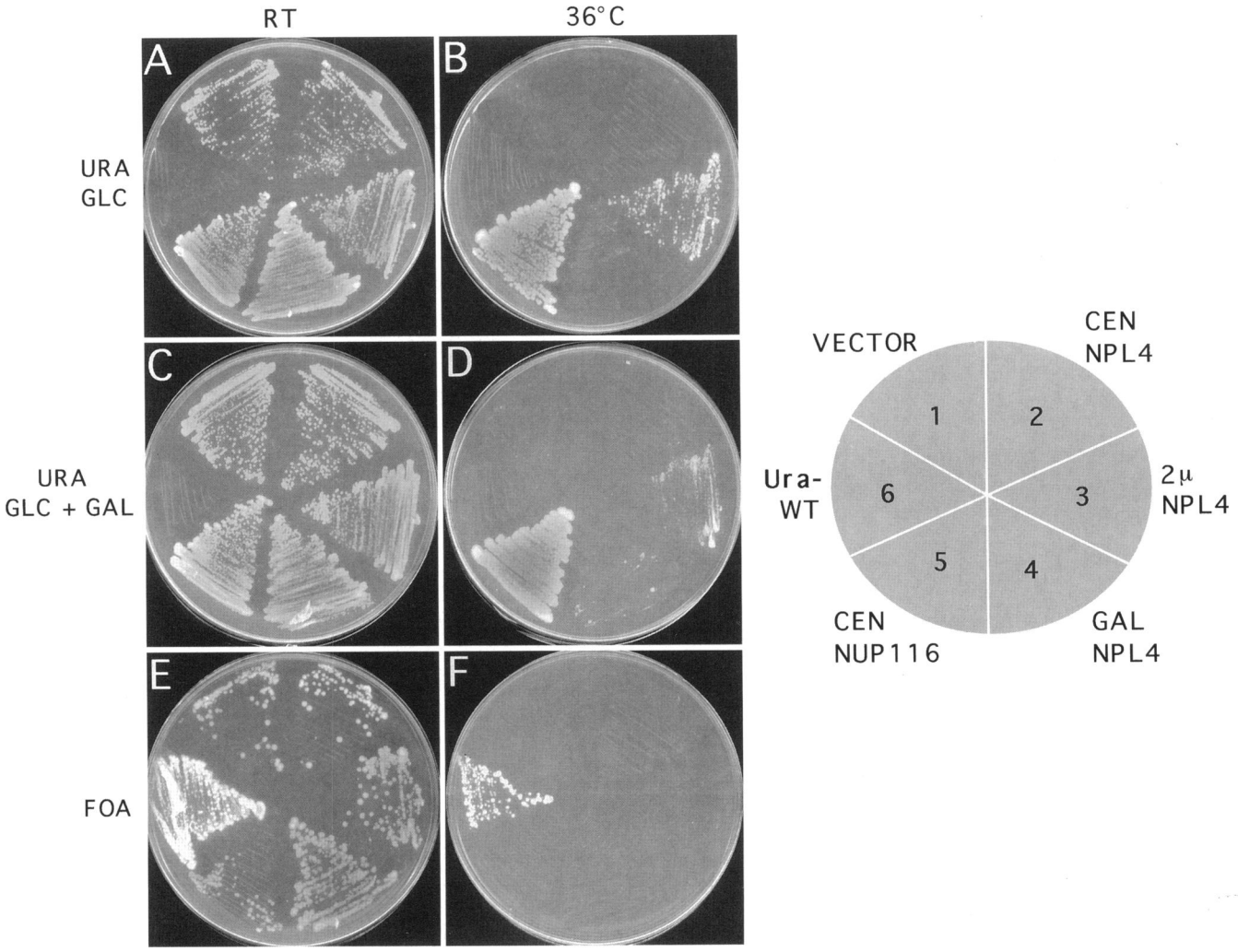

Figure 12. High-copy plasmids containing *NPL4* partly rescue the Δ*nup116* Ts$^-$ defect. The Δ*nup116* strain was transformed with plasmids containing *URA3* (section 1) or single-copy *URA3* and *NPL4* (section 2), high-copy *URA3* and *NPL4* (section 3), *URA3* and *GAL1* promoter-*NPL4* (section 4), or single-copy *URA3* and *NUP116* (section 5). The Δ*nup116* transformants and a Ura$^-$ wild-type strain (section 6) were plated at RT (A, C, and E) and 36°C (B, D, and F) on uracil drop-out plates with glucose (A and B). Ura drop-out plates with glucose and galactose (C and D), and 5-FOA plates (E and F).

Npl4-2 cells have nuclear envelope herniations which appear to be identical to those described for Δ*nup116* cells. This presents the possibility that the nuclear defects of the *npl4* and Δ*nup116* strains are related. The Δ*nup116* herniations have been explained as temperature-sensitive disruptions of interactions between the NPC and an integral membrane protein in the nuclear envelope (Wente and Blobel, 1993). We hypothesize that the *npl4* cells also have temperature-sensitive defects in NPC/nuclear envelope interactions. At the restrictive temperature, *npl4* cells have decreased levels of Npl4p, and NPCs that are deficient for Npl4p may be less tightly bound to the pore membrane. This, in turn, may allow the protrusion of the pore membrane away from the NPC and toward the cytoplasm. In *npl4-1* cells, the pore membrane protrusion might extend from a small segment of the pore membrane that abuts the NPC and result in the formation of a nuclear envelope tail. In *npl4-2* cells, the protrusion might originate from the entire segment of pore membrane surrounding the NPC, fuse over the NPC, and form a nuclear envelope seal. According to this model, Npl4p acts as a NE anchor; Npl4p stabilizes the contact between the pore membrane and the NPC. In agreement with the Npl4p NE anchor model, *npl4* cells contain decreased levels of Npl4p, *npl4-2* cells have lower levels of Npl4p than

npl4-1 cells, and *npl4-2* cells may possibly have more rapid oligomerization or aggregation of Npl4p than *npl4-1* cells.

This model predicts that Npl4p and Nup116p have overlapping functions, which may be observed as genetic interactions. In fact, we did not observe synthetic lethality between the *npl4-2* and Δ*nup116* strains (our unpublished observations). One explanation for this result is that synthetic lethality requires that the double mutant be inviable at the permissive temperature. Since the *npl4-2* and Δ*nup116* cells have no NE herniations at RT (see above; Wente and Blobel, 1993), it is conceivable that the *npl4-2*/Δ*nup116* double mutant is indistinguishable from the single mutants under these conditions. Instead, the *npl4-2*/Δ*nup116* double mutant may have a faster and/or more complete onset of nuclear envelope herniations at the restrictive temperature. Alternately, the *npl4-2*/Δ*nup116* mutant may exhibit nuclear envelope herniations at a semipermissive temperature.

Consistent with the Npl4p NE anchor model, a high-copy plasmid containing *NPL4* can partly rescue the growth and structural defects of the Δ*nup116* strain. This implies that additional copies of the Npl4p can partly substitute for Nup116p. Yet, high-copy plasmids containing *NUP116* fail to rescue the *npl4-1* or *npl4-2* Ts^- defects, indicating that Npl4p and Nup116p are not interchangeable. It is possible that Npl4p and Nup116p have overlapping anchoring functions and separate transport functions. Nup116p appears to be directly involved in RNA export (Fabre *et al.*, 1994) and protein import (Iovine *et al.*, 1995), but the nature of Npl4p's involvement in nuclear transport remains unclear (see below). Interestingly, a plasmid containing *GAL1*-promoter-*NPL4* weakly rescues the Δ*nup116* Ts^- defect in the presence of glucose and galactose and fails to rescue the Δ*nup116* Ts^- defect in the presence of galactose alone. This implies that overexpression of Npl4p inhibits complementation of the Δ*nup116* strain and is consistent with the observation that Npl4p overproduction results in the cytoplasmic localization of the protein (our unpublished observations). It should be noted that a plasmid containing *GAL10* promoter-*NUP116* was not tested for the ability to rescue the *npl4-1* and *npl4-2* Ts^- defects, since overproduction of Nup116p strongly inhibits cell growth (Wente and Blobel, 1993).

Of importance, the *npl4-2*/Δ*nup116* nuclear envelope herniations are distinct from the nuclear envelope blisters observed in *nup188* cells (Nehrbass *et al.*, 1996) and the NPC clusters observed in Δ*nup133*/*rat3-1*, *rat7-1*, Δ*nup120*/*rat2-1*, *rat2-2*, Δ*nup84*, and Δ*nup85*/*rat9-1* cells (Doye *et al.*, 1994; Aitchison *et al.*, 1995b; Gorsch *et al.*, 1995; Heath *et al.*, 1995; Li *et al.*, 1995; Goldstein *et al.*, 1996; Siniossogiou *et al.*, 1996). First, the NPC clusters observed in *nup*/*rat* cells are thought to be caused by improper associations of newly assembled NPCs (Heath *et al.*, 1995). Although the *npl4-2*/Δ*nup116* herniations can group on one side of the nuclear envelope (see above; Wente and Blobel, 1993), it is unlikely that this grouping is caused by new NPCs. This would require that *npl4-2* and Δ*nup116* cells assemble new, interassociating, export-functional NPCs on the nuclear face of the inner nuclear membrane without connections to nuclear membrane channels. In these cells, it is more likely that new NPCs appear normal; according to the *npl4-2* and Δ*nup116* models (see above; Wente and Blobel, 1993), new NPCs would not be immediately sealed by nuclear membrane. Second, the nuclear envelope blisters observed in *nup188* cells and the NPC clusters observed in the *nup*/*rat* cells appear to be unlinked to translocation defects. *Nup188* cells form nuclear envelope blisters at the nonpermissive temperature, but do not display defects in nucleocytoplasmic transport (Nehrbass *et al.*, 1996). *Rat7-1* cells cluster their NPCs and export poly(A)$^+$ RNA normally at the permissive temperature, but distribute their NPCs normally and retain poly(A)$^+$ RNA in the nucleus at the nonpermissive temperature (Gorsch *et al.*, 1995). Δ*Nup133*/*rat3-1*, Δ*nup120*/*rat2-1*, *rat2-2*, Δ*nup84*, and Δ*nup85*/*rat9-1* cells exhibit constitutive NPC clustering but retain poly(A)$^+$ RNA in the nucleus at the nonpermissive temperature (Doye *et al.*, 1994; Aitchison *et al.*, 1995b; Li *et al.*, 1995; Heath *et al.*, 1995; Goldstein *et al.*, 1996; Siniossogiou *et al.*, 1996). In contrast, *npl4-2* and Δ*nup116* cells seal off their NPCs and block protein import (see above) and poly(A)$^+$ RNA export (see above; Wente and Blobel, 1993) at the nonpermissive temperature. Thus, for *npl4-2* and Δ*nup116* cells, the structural and transport defects are linked.

It is not known whether the *npl4-1* transport defects are due to structural defects. *Npl4-1* cells do not accumulate poly(A)$^+$ RNA in the nucleus or form nuclear envelope herniations, but show defects in protein import. It is possible that *npl4-1* cells are directly defective for import. Alternately, *npl4-1* cells may have nuclear envelope alterations that block import, but leave export unaffected. Consistent with this idea, *npl4-1* and *npl4-2* cells show a temporal correlation between structural and transport defects. *Npl4-2* cells exhibit nuclear envelope herniations, nuclear accumulation of poly(A)$^+$ RNA, and nuclear import defects after a 30-min shift to the nonpermissive temperature. *Npl4-1* cells exhibit nuclear envelope projections and significant nuclear import defects after a 3-h shift to the nonpermissive temperature. Yet, even if there is a correlation between *npl4-1* structural and transport defects, it remains unclear as to how nuclear envelope projections could block protein import. One formal possibility is that the *npl4-1* nuclear envelope projections are accompanied by structural alterations that are not visible in our electron micrographs. Finally, it

should be noted that after a 30-min shift to 37°C, ~7% of the *npl4-2* cells exhibit nuclear envelope herniations, whereas ~76% of these cells show nuclear accumulation of poly(A)$^+$ RNA. We hypothesize that there is a lag period between the nuclear envelope sealing and the appearance of nuclear envelope herniations; herniations may appear only after significant amounts of poly(A)$^+$ RNA and export materials have accumulated and distended the membrane seal.

The localization of Npl4p and the functional and structural defects of the *npl4* cells strongly suggest that *NPL4* encodes a novel yeast nucleoporin or NPC-associated protein involved in the maintenance of nuclear structure and function. Npl4p is notable in that it is the first NPC or NPC-associated protein identified by a genetic screen for nuclear localization components. As such, it validates the *npl* screen and provides a pathway for the discovery of additional NPC, nuclear envelope, and/or nuclear transport components.

ACKNOWLEDGMENTS

We thank Yuhui Xu for expert and extensive assistance in electron microscopy; Charles Cole and Gabriel Schlenstedt for strains, reagents, and critical readings of this manuscript; Susan Wente and Richard Wozniak for providing strains and plasmids; and Michael Henry, David Pellman, and Laura Davis for helpful suggestions. This work was supported by grants from the National Institutes of Health to P.A.S. C.D. was supported in part by a National Institutes of Health Cancer training grant and a Markey Foundation predoctoral fellow grant to Princeton University.

REFERENCES

Aebi, M., Clark, M.W., Vijayraghavan, U., and Abelson, J. (1990). A yeast mutant, *PRP20*, altered in mRNA metabolism and maintenance of the nuclear structure, is defective in a gene homologous to the human gene *RCC1* which is involved in the control of chromosomal condensation. Mol. Gen. Genet. *224*, 72–80.

Aitchison, J.D., Blobel, G., and Rout, M.P. (1995a). Nup120p: a yeast nucleoporin required for NPC distribution and mRNA transport. J. Cell Biol. *131*, 1659–1675.

Aitchison, J.D., Rout, M.P., Marelli, M., Blobel, G., and Wozniak, R.W. (1995b). Two novel related nucleoporins Nup170p and Nup157p: complementation with the vertebrate homologue Nup155p and functional interactions with the yeast nuclear pore-membrane protein Pom152p. J. Cell Biol. *131*, 1133–1148.

Amberg, D.C., Fleischmann, M., Stagljar, I., Cole, C.N., and Abei, M. (1993). Nuclear Prp20 protein is required for mRNA export. EMBO J. *12*, 233–241.

Amberg, D.C., Goldstein, A.L., and Cole, C.N. (1992). Isolation and characterization of *RAT1*, an essential gene in *Saccharomyces cerevisiae* required for the efficient nucleocytoplasmic trafficking of mRNA. Genes Dev. *9*, 1173–1189.

Anderson, J.T., Wilson, S.M., Datar, K.V., and Swanson, M.S. (1993). Nab2, a yeast polyadenylated RNA-binding protein essential for cell viability. Mol. Cell. Biol. *13*, 2730–2741.

Aris, J.P., and Blobel, G. (1989). Yeast nuclear envelope proteins cross react with an antibody against mammalian pore complex proteins. J. Cell Biol. *108*, 2059–2067.

Bischoff, F.R., Krebber, H., Kempf, T., Hermes, I., and Ponstingl, H. (1995a). Human RanGTPase-activating protein RanGAP1 is a homologue of yeast Rna1p involved in mRNA processing and transport. Proc. Natl. Acad. Sci. USA *92*, 1749–1753.

Bischoff, F.R., Krebber, H., Smirnova, E., Dong, W., and Postingl, H. (1995b). Co-activation of RanGTPase and inhibition of GTP dissociation by Ran-GTP binding protein RanBP1. EMBO J. *14*, 705–715.

Bischoff, F.R., and Ponstingl, H. (1991). Catalysis of guanine nucleotide exchange on Ran by the mitotic regulator RCC1. Nature *354*, 80–82.

Bogerd, A.M., Hoffman, J.A., Amberg, D.C., Fink, G.R., and Davis, L.I. (1994). Nup1 mutants exhibit pleotropic defects in nuclear pore complex function. J. Cell Biol. *127*, 319–332.

Bonneaud, N., Minville-Sebastia, L., Cullin, C., and Lacroute, F. (1994). Cellular localization of Rna14p and Rna15p, two yeast proteins involved in mRNA stability. J. Cell Sci. *107*, 913–921.

Bossie, M.A., DeHoratius, C., Barcelo, G., and Silver, P. (1992). A mutant nuclear protein with similarity to RNA binding proteins interferes with nuclear import in yeast. Mol. Biol. Cell *3*, 875–893.

Butler, G., and Wolfe, K.H. (1994). Yeast homologue of mammalian Ran binding protein 1. Biochim. Biophys. Acta *1219*, 711–712.

Chiang, A.N. (1993). Isolation and Characterization of Mutants That Affect Nuclear Protein Localization. Ph.D. Thesis. Princeton, NJ: Princeton University, 80–105.

Corbett, A.H., Koepp, D.M., Schlenstedt, G., Lee, M.S., Hopper, A.K., and Silver, P.A. (1995). Rna1p, a Ran/TC4 GTPase activating protein, is required for nuclear import. J. Cell Biol. *130*, 1017–1026.

Corbett, A.H., and Silver, P.A. (1996). The *NTF2* gene encodes an essential, highly conserved protein that functions in nuclear transport in vivo. J. Biol. Chem. *271*, 18477–18484.

Coutavas, E., Ren, M., Oppenheim, J.D., Eustachio, P.D., and Rush, M.G. (1993). Characterization of proteins that interact with the cell-cycle regulatory protein Ran/TC4. Nature *366*, 585–587.

Davis, L.I. (1995). The nuclear pore complex. Annu. Rev. Biochem. *64*, 865–896.

Deshaies, R.J., and Schekman, R. (1987). A yeast mutant defective at an early stage in import of secretory protein precursors into the endoplasmic reticulum. J. Cell Biol. *105*, 633–646.

Deshaies, R.J., and Schekman, R. (1989). SEC62 encodes a putative membrane protein required for protein translocation into the yeast endoplasmic reticulum. J. Cell Biol. *109*, 2653–2664.

Doye, V., and Hurt, E.C. (1995). Genetic approaches to nuclear pore structure and function. Trends Genet. *11*, 235–241.

Doye, V., Wepf, R., and Hurt, E.C. (1994). A novel nuclear pore protein Nup133p with distinct roles in poly(A)$^+$ RNA transport and nuclear pore distribution. EMBO J. *13*, 6062–6075.

Emr, S.D., Vassarotti, A., Garrett, J., Geller, B.L., Takeda, M., and Douglas, M.G. (1986). The amino terminus of the yeast FI-ATPase beta-subunit precursor functions as a mitochondrial import signal. J. Cell Biol. *102*, 523–533.

Fabre, E., Boelens, W.C., Wimmer, C., Mattaj, I.W., and Hurt, E.C. (1994). Nup145p is required for nuclear export of mRNA and binds homopolymeric RNA in vitro via a novel conserved motif. Cell *78*, 275–289.

Flach, J., Bossie, M., Vogel, J., Corbett, A., Jinks, T., Willins, D., and Silver, P.A. (1994). A yeast RNA binding protein shuttles between the nucleus and the cytoplasm. Mol. Cell. Biol. *14*, 8399–8407.

Fleischmann, M., Clark, M.W., Forrester, W., Wickens, M., Nishimoto, T., and Aebi, M. (1991). Analysis of the yeast prp20 mutations and functional complementation by the human homologue RCC1, a

protein involved in the control of chromosome condensation. Mol. Gen. Genet. *227*, 417–423.

Fritz, C.C., and Green, M.R. (1996). HIV Rev uses a conserved cellular protein export pathway for the nucleocytoplasmic transport of viral mRNAs. Curr. Biol. *6*, 848–854.

Gietz, D., Jean, A.S., Woods, A., and Schiestl, R.H. (1992). Improved methods for high efficiency transformation of intact yeast cells. Nucleic Acids Res. *20*, 1425.

Goldberg, M.W., and Allen, T.D. (1995). Structural and functional organization of the nuclear envelope. Curr. Opin. Cell Biol. *7*, 301–309.

Goldstein, A.L., Snay, C.A., Heath, C.V., and Cole, C.C. (1996). Pleotropic nuclear defects associated with a conditional allele of the novel nucleoporin Rat9p/Nup85p. Mol. Biol. Cell *7*, 917–934.

Görlich, D., and Mattaj, I.W. (1996). Nucleocytoplasmic transport. Science *271*, 1513–1518.

Görlich, D., Vogel, F., Millis, A.D., Hartmann, E., and Laskey, R.A. (1995). Distinct functions for the two importin subunits in nuclear protein import. Nature *377*, 246–248.

Gorsch, L.C., Dockendorff, T.C., and Cole, C.N. (1995). A conditional allele of the repeat-containing yeast nucleoporin *RAT7/NUP159* causes both rapid cessation of mRNA export and reversible clustering of the nuclear pore complexes. J. Cell Biol. *129*, 939–955.

Grandi, P., Emig, S., Weise, C., Hucho, F., Pohl, T., and Hurt, E.C. (1995). A novel nuclear pore protein Nup82p which specifically binds to Nsp1p. J. Cell Biol. *130*, 1263–1273.

Hallberg, E., Wozniak, R.W., and Blobel, G. (1993). An integral membrane protein of the pore membrane domain of the nuclear envelope contains a nucleoporin-like region. J. Cell Biol. *122*, 513–521.

Heath, C.V., Copeland, C.S., Amberg, D.C., Priore, V.D., Snyder, M., and Cole, C.N. (1995). Nuclear pore complex clustering and nuclear accumulation of poly(A)$^+$ RNA associated with mutation of the *Saccharomyces cerevisiae RAT2/NUP120* gene. J. Cell Biol. *131*, 1677–1697.

Henry, M., Borland, C.Z., Bossie, M., and Silver, P.A. (1996). Potential RNA-binding proteins in *Saccharomcyes cerevisiae* identified as suppressors of temperature-sensitive mutations in *NPL3*. Genetics *142*, 103–115.

Hopper, A.K., Traglia, H.M., and Dunst, R.W. (1990). The yeast *RNA1* gene product necessary for RNA processing is located in the cytosol and apparently excluded from the nucleus. J. Cell Biol. *111*, 309–321.

Huang, S., Deernick, T.J., Ellisman, M.H., and Spector, D.L. (1994). In vivo analysis of the stability and transport of poly(A)$^+$ RNA. J. Cell Biol. *126*, 877–899.

Hurwitz, M.E., and Blobel, G. (1995). NUP82 is an essential yeast nucleoporin required for poly(A)$^+$ RNA export. J. Cell Biol. *130*, 1275–1281.

Iovine, K.M., Watkins, J.L., and Wente, S.R. (1995). The GLFG repetitive region of the nucleoporin Nup116p interacts with Kap95p, an essential yeast nuclear import factor. J. Cell Biol. *131*, 1699–1713.

Ito, H., Fukado, Y., Murata, K., and Kimura, A. (1983). Transformation of intact yeast cells with alkali cations. J. Bacteriol. *153*, 163–168.

Izzurralde, E., and Mattaj, I.W. (1995). RNA export. Cell *81*, 153–159.

Jones, J.S., and Prakash, L. (1990). Yeast *Saccharomyces cerevisiae* selectable markers in pUC18 polylinkers. Yeast *6*, 363–366.

Kadowaki, T., Goldfarb, D., Spitz, L.M., Tartakoff, A.M., and Ohno, M. (1993). Regulation of RNA processing and transport by a nuclear guanine nucleotide release protein and members of the Ras superfamily. EMBO J. *12*, 2929–2937.

Kadowaki, T., Zhou, Y., and Tartakoff, A. (1992). A conditional yeast mutant deficient in mRNA transport from nucleus to cytoplasm. Proc. Natl. Acad. Sci. USA *89*, 2312–2316.

Kassir, Y., and Simchen, G. (1991). Monitoring Meiosis and Sporulation in *Saccharomyces cerevisiae*, San Diego, CA: Academic Press.

Klyce, H.R., and McLaughlin, C.S. (1973). Characterization of temperature-sensitive mutants of yeast by a photomicrographic procedure. Exp. Cell Res. *82*, 47–56.

Koepp, D., Wong, D.H., Corbett, A.H., and Silver, P.A. (1996). Dynamic localization of the nuclear import receptor and its interactions with transport factors. J. Cell Biol., *133*, 1163–1176.

Kraemer, D., Wozniak, R.W., Blobel, G., and Radu, A. (1994). The human CAN protein, a putative oncogene product associated with myeloid leukemogenesis, is a nuclear pore complex protein that faces the cytoplasm. Proc. Natl. Acad. Sci. USA *91*, 1519–1523.

Laemmli, U.K. (1970). Cleavage of structural proteins during assembly of the head of bacteriophage T4. Nature *227*, 680–685.

Lee, M.S., Henry, M., and Silver, P.A. (1996). A protein that shuttles between the nucleus and the cytoplasm is an important mediator of RNA export. Genes Develop. *10*, 1233–1246.

Li, O., Heath, C.V., Amberg, D.C., Dockendorff, T.C., Copeland, C.S., Snyder, M., and Cole, C.N. (1995). Mutation or deletion of the *Saccharomyces cerevisiae RAT3/NUP133* gene causes temperature-dependent nuclear accumulation of poly(A)$^+$ RNA and constitutive clustering of nuclear pore complexes. Mol. Biol. Cell *6*, 401–417.

Loeb, J.D.J., Schlenstedt, G., Pellman, D., Kornitzer, D., Silver, P.A., and Fink, G.R. (1995). The yeast nuclear import receptor is required for mitosis. Proc. Natl. Acad. Sci. USA 7647–7651.

McDonald, K. (1984). Osmium ferricyanide fixation improves microfilament preservation and membrane visualization in a variety of animal cells. J. Ultrastruct. Res. *86*, 107–118.

Melchior, F., and Gerace, L. (1995b). Mechanisms of nuclear protein import. Curr. Opin. Cell Biol. *7*, 310–318.

Melchior, F., Guan, T., Yokoyama, N., Nishimoto, T., and Gerace, L. (1995a). GTP hydrolysis by Ran occurs at the nuclear pore complex in an early step of protein import. J. Cell Biol. *131*, 571–581.

Melchior, F., Paschal, B., Evans, J., and Gerace, L. (1993). Inhibition of nuclear protein import by nonhydrolyzable analogues of GTP and identification of the small GTPase Ran/TC4 as an essential transport factor. J. Cell Biol. *123*, 1649–1659.

Moore, M.S., and Blobel, G. (1993). The GTP-binding protein Ran/TC4 is required for protein import into the nucleus. Nature *365*, 661–663.

Moore, M.S., and Blobel, G. (1994). Purification of a Ran-interacting protein that is required for protein import into the nucleus. Proc. Natl. Acad. Sci. USA *91*, 10212–10216.

Moreland, R.B., Langevin, G.L., Singer, H.R., Garcea, R.L., and Hereford, L.M. (1987). Amino acid sequences that determine the nuclear localization of yeast histone 2B. Mol. Cell. Biol. *7*, 4048–4057.

Moroianu, J., Blobel, G., and Radu, A. (1995a). Previously identified protein of uncertain function is karyopherin α and together with karyopherin β docks import substrate at nuclear pore complexes. Proc. Natl. Acad. Sci. USA *92*, 2008–2011.

Moroianu, J., Hijkata, M., Blobel, G., and Radu, A. (1995b). Mammalian karyopherin $\alpha_1\beta$ and $\alpha_2\beta$ heterodimers: α_1 or α_2 subunit binds nuclear localization signal and β subunit interacts with peptide repeat-containing nucleoporins. Proc. Natl. Acad. Sci. USA *92*, 6532–6536.

Nehrbass, U., and Blobel, G. (1996). Role of the nuclear transport factor p10 in nuclear import. Science *272*, 120–122.

Nehrbass, U., Rout, M.P., Maguire, S., Blobel, G., and Wozniak, R.W. (1996). The yeast nucleoporin Nup188 interacts genetically and physically with the core structures of the nuclear pore complex. J. Cell Biol. *133*, 1153–1162.

Nelson, M., and Silver, P. (1989). Context affects nuclear protein localization in *Saccharomyces cerevisiae*. Mol. Cell. Biol. *9*, 384–389.

Ng, T.W.D., and Walter, P. (1996). ER membrane protein complex required for nuclear fusion. J. Cell Biol. *132*, 499–509.

Orr-Weaver, T.L., and Szostak, J.W. (1983). Yeast recombination: the association between double-stranded gap-repair and crossing over. Proc. Natl. Acad. Sci. USA *80*, 4417–4421.

Paschal, B.M., and Gerace, L. (1995). Identification of NTF2, a cytosolic factor for nuclear import that interacts with nuclear pore complex protein p62. J. Cell Biol. *129*, 925–937.

Powers, M.A., and Forbes, D.J. (1994). Cytosolic factors in nuclear transport: what's importin? Cell *79*, 931–934.

Radu, A., Blobel, G., and Moore, M.S. (1995a). Identification of a protein complex that is required for nuclear protein import and mediates docking of import substrate to distinct nucleoporins. Proc. Natl. Acad. Sci. USA *92*, 1769–1773.

Radu, A., Moore, M.S., and Blobel, G. (1995b). The peptide repeat domain of nucleoporin Nup98 functions as a docking site in transport across the nuclear pore complex. Cell *81*, 215–222.

Rexach, M., and Blobel, G. (1995). Protein import into nuclei: association and dissociation reactions involving transport substrate, transport factors, and nucleoporins. Cell *83*, 683–692.

Rose, M.D., Novick, P., Thomas, J.H., Botstein, D., and Fink, G.R. (1987). A *Saccharomyces cerevisiae* genomic plasmid bank based on a centromere-containing shuttle vector. Gene *60*, 237–243.

Rose, M.D., Winston, F., and Hieter, P. (1990). Methods in Yeast Genetics: a Laboratory Course Manual, Cold Spring Harbor, NY: Cold Spring Harbor Laboratory Press.

Rothblatt, J.A., Deshaies, R.J., Sanders, S.L., Daum, G., and Schekman, R. (1989). Multiple genes are required for proper insertion of secretory proteins into the endoplasmic reticulum in yeast. J. Cell Biol. *109*, 2641–2652.

Rout, M.P., and Blobel, G. (1993). Isolation of the yeast nuclear pore complex. J. Cell Biol. *123*, 771–783.

Rout, M.P., and Wente, S.R. (1994). Pores for thought: nuclear pore complex proteins. Trends Cell Biol. *4*, 357–365.

Sadler, I., Chiang, A., Kurihara, T., Rothblatt, J., Way, J., and Silver, P. (1989). A yeast gene important for protein assembly into the endoplasmic reticulum and the nucleus has homology to DnaJ, an *Escherichia coli* heat shock protein. J. Cell Biol. *109*, 2665–2675.

Sanger, F., Nicklen, S., and Coulson, A.R. (1977). DNA sequencing with chain terminating inhibitors. Proc. Natl. Acad. Sci. USA *74*, 5463–5467.

Schaaff-Gerstenschläger, I., Baur, A., Boles, E., and Zimmermann, F.K. (1993). Sequence and function analysis of a 4.3 kb fragment of *Saccharomyces cerevisiae* chromosome II including three open reading frames. Yeast *9*, 915–921.

Schlenstedt, G., Hurt, E., Doye, V., and Silver, P.A. (1993). Reconstitution of nuclear protein transport with semi-intact yeast cells. J. Cell Biol. *123*, 785–798.

Schlenstedt, G., Saavedra, C., Loeb, J.D.J., Cole, C.N., and Silver, P.A. (1995a). The GTP-bound form of the yeast Ran/TC4 homolog blocks nuclear protein import and appearance of poly(A)$^+$ RNA in the cytoplasm. Proc. Natl. Acad. Sci. USA *92*, 225–229.

Schlenstedt, G., Wong, D.H., Koepp, D.M., and Silver, P.A. (1995b). Mutants in a yeast Ran binding protein are defective in nuclear transport. EMBO J. *14*, 101–112.

Siniossogiou, S., Wimmer, C., Rieger, M., Doye, V., Tekotte, H., Weise, C., Emig, S., Segref, A., and Hurt, E.C. (1996). A novel complex of nucleoporins, which includes Sec13p and a Sec13p homolog, is essential for normal nuclear pores. Cell *84*, 265–275.

Stutz, F., Neville, M., and Rosbash, M. (1995). Identification of a novel nuclear pore-associated protein as a functional target of the HIV-1 Rev protein in yeast. Cell *82*, 495–506.

Sukegawa, J., and Blobel, G. (1993). A nuclear pore complex protein that contains zinc finger motifs, binds DNA, and faces the nucleoplasm. Cell *72*, 29–38.

Sweet, D.J., and Gerace, L. (1995). Taking from the cytoplasm and giving to the pore: soluble factors in nuclear protein import. Trends Cell Biol. *5*, 444–447.

Tachibana, T., Imamoto, N., Seino, H., Nishimoto, T., and Yoneda, Y. (1994). Loss of RCC1 leads to suppression of nuclear protein import in living cells. J. Biol. Chem. *269*, 24542–24545.

Tani, T., Derby, R.J., Hiraoka, Y., and Spector, D.L. (1995). Nucleolar accumulation of poly(A)$^+$ RNA in heat-shocked yeast cells: implication of nucleolar involvement in mRNA transport. Mol. Biol. Cell *6*, 1515–1534.

Thomas, B.J. and Rothstein, R. (1989). Elevated recombination rates in transcriptionally active DNA. Cell *56*, 619–630.

von Lindern, M., Fornerod, M., Baal, S.v., Jaegle, M., Wit, T.d., Buijs, A., and Grosveld, G. (1992). The translocation (6;9), associated with a specific subtype of acute myeloid leukemia, results in the fusion of two genes, *dek* and *can*, and the expression of a chimeric, leukemia-specific *dek-can* mRNA. Mol. Cell. Biol. *12*, 1687–1697.

Wente, S.R., and Blobel, G. (1993). A temperature-sensitive NUP116 null mutant forms a nuclear envelope seal over the yeast nuclear pore complex thereby blocking nucleocytoplasmic traffic. J. Cell Biol. *123*, 275–284.

Wente, S.R., and Blobel, G. (1994). NUP145 encodes a novel yeast glycine-leucine-phenylalanine-glycine (GLFG) nucleoporin required for nuclear envelope structure. J. Cell Biol. *125*, 955–969.

Wente, S.R., Rout, M.P., and Blobel, G. (1992). A new family of yeast nuclear pore complex proteins. J. Cell Biol. *119*, 705–723.

Wilson, S.M., Datal, K.V., Paddy, M.R., Swedlow, J.R., and Swanson, M. (1994). Characterization of nuclear polyadenylated RNA-binding proteins in *Saccharomyces cerevisiae*. J. Cell Biol. *127*, 1173–1184.

Wu, J., Matunis, M.J., Kraemer, D., Blobel, G., and Coutavas, E. (1995). Nup358, a cytoplasmically exposed nucleoporin with peptide repeats, Ran-GTP binding sites, zinc fingers, a cyclophilin A homologous domain, and a leucine-rich region. J. Biol. Chem. *270*, 14209–14213.

Yokoyama, N., Hayashi, N., Seki, T., Pantè, N., Ohba, T., Nishii, K., Kuma, K., Hayashida, T., Miyata, T., Aebi, U., Fukui, M., and Nishimoto, T. (1995). A giant nucleopore protein that binds Ran/TC4. Nature *376*, 184–188.

Zabel, U., Doye, V., Tekotte, H., Wepf, R., Grandi, P., and Hurt, E.C. (1996). Nic96p is required for nuclear pore formation and functionally interacts with a novel nucleoporin, Nup188. J. Cell Biol. *133*, 1141–1152.